Ref
T
E443

V.6 #1

ELECTRONIC PROGRESS

RAYTHEON

FEB 21 1962
LIBRARY

NOVEMBER-DECEMBER 1961

in this issue:

INTERPLANETARY TRANSFER

VOLUME VI NOVEMBER-DECEMBER 1961 NUMBER 3

ELECTRONIC PROGRESS

RAYTHEON

1 Characteristics of a Backward-Wave Oscillator with an External Feedback Circuit . . . . . *Samuel J. Ameen, Robert Plumridge*

8 A Design Technique for High Speed Transistor Circuits . . . . . *Walter A. Doesschate, Jr.*

14 Principles of Astronautics . . . . *Gerald A. Ouellette*
3. Interplanetary Transfer

22 A Symbol Generator for Air Traffic Control . . . . . *Raymond W. Dankwardt*

24 Notes on Patents, Papers and Publications

Martin Schilling . . . . . **EXECUTIVE EDITOR**
Michael A. Walker . . . . . **MANAGING EDITOR**
Mary F. Sullivan . . . . . **EDITOR**
William Niles . . . . . **ART EDITOR**

Printed in U.S.A. Copyright 1962, Raytheon Company, Lexington, Mass.

EDITORIAL ADVISORY BOARD

Laurence Batchelder
Submarine Signal Operation
Robert Edwards
Microwave and Power Tube Division
John D. Harmer
Missile and Space Division
John S. MacDougall
Semiconductor Division
Peter Nutter
Research Division
Gordon R. Partridge
Communications and Data Processing Operation
Robert L. Wyckoff
Surface Radar and Navigation Operation

COVER

As the barriers to space flight are surmounted one by one, man's age-old desire to visit the planets comes closer to reality. In this issue the problem of interplanetary transfer is discussed in the third article of a five-part series on Astronautics.

QKB 924

CHARACTERISTICS OF A BACKWARD-WAVE OSCILLATOR WITH AN EXTERNAL FEEDBACK CIRCUIT

by SAMUEL J. AMEEN and ROBERT PLUMRIDGE

THE conventional "O" type backward-wave oscillator (BWO) is an electronically tunable, self-excited oscillator whose oscillator frequency varies continuously as the beam voltage is changed.[1]

When the backward-wave oscillator is modified so that part of the power output is fed back, the device has new characteristics, i.e., operation occurs only at discrete frequencies as the beam voltage is varied. The resulting tuning curve has a staircase appearance, and the oscillation frequency on any one of the steps is extremely stable. This device is well suited for applications where rapid switching over a large frequency band may be required such as frequency diversity radar.

This paper presents results obtained on a Raytheon S-band BWO employing an interdigital delay line structure and a $\frac{5}{8}$ inch diameter styroflex coaxial cable as the feedback circuit. Testing was done mainly in the 2700-3000 Mc range since this band was of greatest interest although the tube is capable of operation over the 2000-4000 Mc range.

Description of "O" Type BWO

The "O" type BWO is a microwave tube which generates power by the interaction of an electron beam traveling close to a backward slow-wave structure. A schematic of the essential components of this tube is shown in Figure 1.

[1]D. A. Dunn, "Understanding the Backward Wave Oscillator," Electronic Industries (January 1958).

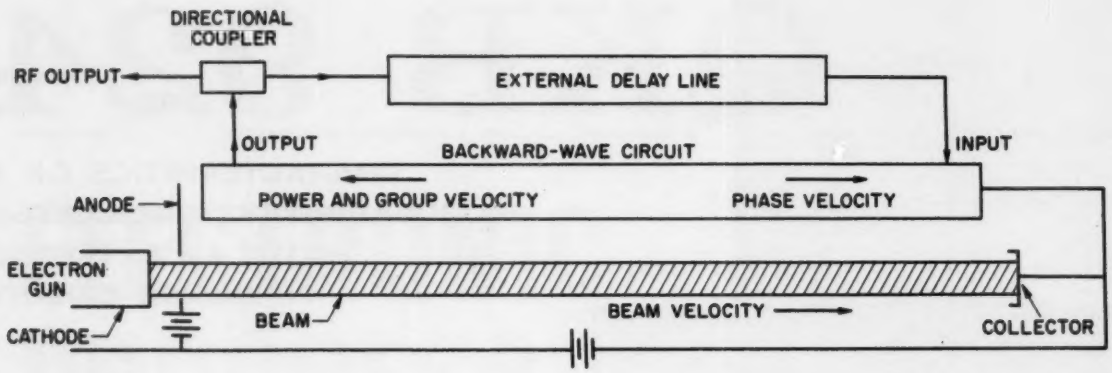

Figure 1. Backward-wave oscillator with external feedback circuit

In this device power fed in at the collector end will be amplified in traveling toward the output at the gun end of the tube. Oscillations occur when the circuit is properly terminated at each end and sufficient beam current is supplied. The oscillation results from a process of continuous feedback because of the interaction of the beam and the rf circuit, and does not depend on reflections from the ends of the circuit.

A circuit having oppositely directed group and phase velocities has the property that the phase velocity varies continuously with frequency. As a result, this type of oscillator tunes continuously over the frequency range of the circuit when the beam voltage is varied.

The Raytheon "O" type BWO's employ an interdigital delay line as the slow-wave structure. The circuit will support this type of -1 backward-wave space harmonic.[2] Oscillations occur when the electron velocity is very nearly that of the phase velocity of the -1 space harmonic.

For the interdigital delay line, the synchronous condition is defined by:

$$\frac{c}{u_o} = \frac{\lambda_o}{2p} - \frac{L+p}{p},$$

where c is the speed of light, u_o the electron velocity, λ_o the free space wavelength, p the pitch of the delay line, and L the finger length. Since u_o is proportional to the applied voltage, this equation can be rewritten as:

$$\frac{506}{\sqrt{V}} = \frac{\lambda_o}{2p} - \frac{L+p}{p}.$$

This equation defines the frequency versus voltage characteristics of a BWO employing an interdigital delay line as the slow-wave structure.

Normally, the delay line structure of the BWO is terminated at the collector end by a matched circuit to make the BWO operation independent of the external load. To introduce feedback into a BWO, the matched termination is removed and a connection is made to the slow-wave structure at the collector end. (See Figure 2.)

The slow-wave structure is now connected at both ends by 50-ohm coaxial lines. The power output is coupled out from the gun end of the slow-wave structure and part of this power output is fed back through a long transmission line to the collector end of the slow-wave structure. Figure 3 is a block diagram of the test setup including the tube and feedback loop.

Analysis of this loop,[3] comprised of the BWO and transmission line, shows that at certain frequencies the power fed back is in such a phase as to re-enforce the wave on the interdigital line, and at others the power

[2]R. Warnecke, P. Guenard and O. Doehler, "Fundamental Phenomena in Traveling-Wave Tubes," Onde Elect. *34*, 323-38 (April 1954). In French.

[3]F. L. Vernon, "The Behavior of a BWO with External Feedback," IRE National Convention Record, 91-102 (1957).

SAMUEL J. AMEEN *is an Engineering Section Head in the Microwave Tube Laboratory of the Microwave and Power Tube Division. Since joining Raytheon as a development engineer in 1950, he has been concerned with the development of wide range, low and high power CW magnetrons, low and high power pulsed magnetrons, ruggedized pulsed magnetrons and backward-wave oscillators. In his present position, Mr. Ameen has supervised a number of magnetron research and development and backward-wave oscillator programs. He received a B.S. in electrical engineering from the University of Massachusetts and an M.S. in electrical engineering from Northeastern University. Mr. Ameen is a registered professional engineer in Massachusetts.*

ROBERT PLUMRIDGE *is a Senior Engineer in the Microwave Tube Laboratory of the Microwave and Power Tube Division. With Raytheon since 1951, he has participated in the development of many types of microwave power tubes, including CW and pulsed magnetrons, monofiers, CW klystrons, backward-wave oscillators, amplitrons and stabilitrons. From 1946-1948 he served as Assistant Chief Chemist at the Hamilton Standard Company; and from 1948-1950 he was a Senior Chemical Engineer at Sylvania Electric Company. Mr. Plumridge received a B.S. in ceramic engineering from Alfred University; an M.S. in physics from Boston University; and has done graduate study toward a Ph.D. in physics from Boston University.*

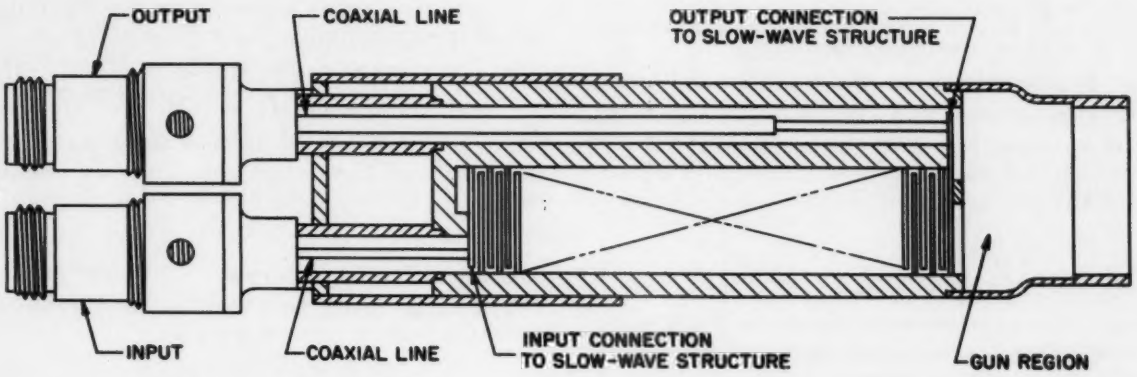

Figure 2. Cross section of QKB 924 BWO

is fed back at a phase which tends to cancel the wave on the slow-wave structure.

The necessary condition for oscillation of a BWO with an external loop circuit can be expressed as

$$GH = 1 \quad . \tag{1}$$

G is the gain of the BWO and it is a function of Pierce's parameters b, QC, CN, and d, while H is a complex function of the external circuit. This function completely describes the frequency characteristics of the external circuit. The gain of the backward-wave oscillator can be written as follows:

$$\frac{1}{G} = \sum \frac{\delta_i^2 + 4\,GC}{(\delta_i - \delta_j)\,(\delta_i - \delta_k)}\, e^{2\pi CN\delta_i}\ e^{-j2\pi N} \quad . \tag{2}$$

The summation of Equation 2 is performed over i = 1, j = 2, K = 3 and cyclic permutation.

Also, the δ's are related to Pierce's parameter by

$$\delta^2 = \frac{1}{b + id - i\,\delta} - 4\,QC \quad , \tag{3}$$

where

$N = \dfrac{\beta_e\, L}{2\pi}$ length of tube in wavelengths

$\beta_e = \omega/u_o$ electron phase constant

L = length of backward-wave oscillator delay line

$\eta = 2\,\pi\,CN$

$C = \left(\dfrac{KI_o}{4V_o}\right)^{1/2}$ Pierce's C parameter

$b = \dfrac{\beta_{-1} - \beta_e}{\beta_e\, C}$

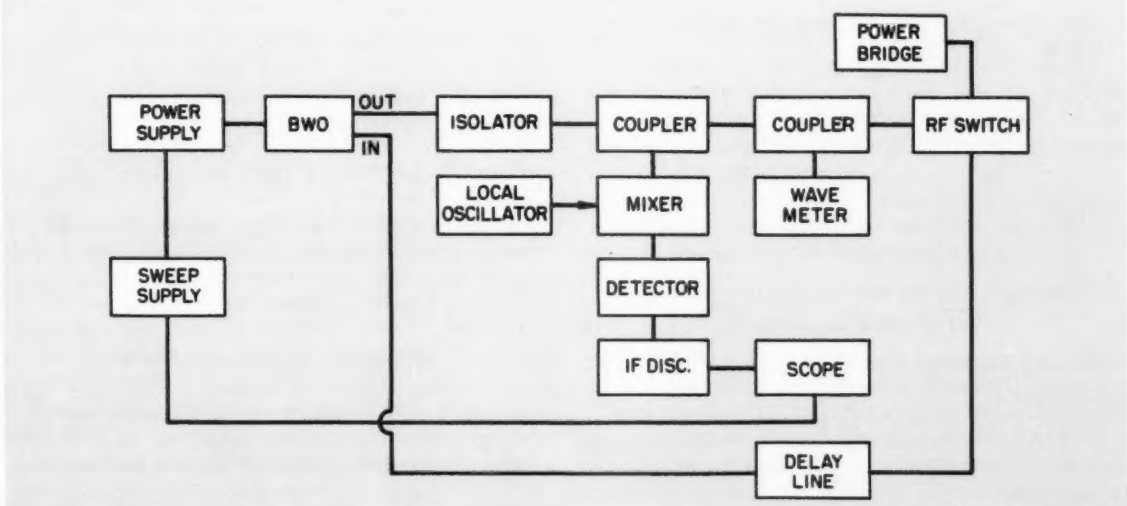

Figure 3. Test setup of QKB 924 BWO

β_{-1} = phase constant of -1 space harmonic

QC = Pierce space charge parameter

d = circuit loss parameter.

Equation 2 has been solved for many combinations of parameters for a BWO with infinite gain ($1/G = 0$). In this analysis the reciprocal of the gain is expanded about b_o and η_o for which the gain is infinite. Therefore:

$$\frac{1}{G} = \left.\frac{\partial\left(\frac{1}{G}\right)}{\partial b}\right|_{b_o,\,\eta_o} \Delta b + \left.\frac{\partial\left(\frac{1}{G}\right)}{\partial \eta}\right|_{b_o,\,\eta_o} \Delta\eta \quad . \quad (4)$$

Next consider the matrix representation of a backward-wave oscillator and the associated transmission line for a feedback circuit. This circuit can be represented as in Figure 4.

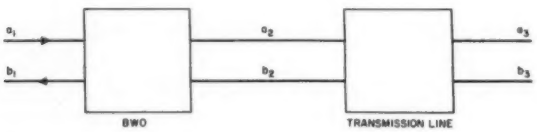

Figure 4. Equivalent circuit for BWO and transmission line

The transmission matrices for each of the components are:

$$T_{BWO} = \begin{pmatrix} G & 0 \\ 0 & e^{+\Gamma^- L} \end{pmatrix} T_{line} = \begin{pmatrix} e^{-\gamma^+ l} & 0 \\ 0 & e^{+\gamma^- l} \end{pmatrix} . \quad (5)$$

The complete matrix transformation for the circuit is:

$$\begin{pmatrix} a_3 \\ b_3 \end{pmatrix} = \begin{pmatrix} e^{-\gamma^+ l} & 0 \\ 0 & e^{+\gamma^- l} \end{pmatrix} \begin{pmatrix} G & 0 \\ 0 & e^{+\Gamma^- L} \end{pmatrix} \begin{pmatrix} a_1 \\ b_1 \end{pmatrix}$$

$$= \begin{pmatrix} Ge^{-\gamma^+ l} & 0 \\ 0 & e^{+\Gamma^- L + \gamma^- l} \end{pmatrix} \begin{pmatrix} a_1 \\ b_1 \end{pmatrix} \quad . \quad (6)$$

Thus, the oscillation conditions are arrived at by requiring:

$$a_3 = a_1$$

$$b_3 = b_1$$

or

$$\begin{pmatrix} Ge^{-\gamma^+ l} - 1 & 0 \\ 0 & e^{\Gamma^- L + \gamma^- l} - 1 \end{pmatrix} \begin{pmatrix} a_1 \\ b_1 \end{pmatrix} = 0 \quad . \quad (7)$$

Hence,

$$(Ge^{-\gamma^+ l} - 1)\ (e^{\Gamma^- L + \gamma^- l} - 1) = 0 \quad . \quad (8)$$

Now expressing the external function H as:

$$H = e^{-\gamma^+ l} = e^{-\alpha^+ l}\, e^{-j\phi} \quad (9)$$

and using Equations 1 and 4, then

$$\left.\frac{\partial}{\partial b}\left(\frac{1}{G}\right)\right|_{b_o,\,\eta_o} \Delta b + \left.\frac{\partial}{\partial \eta}\left(\frac{1}{G}\right)\right|_{b_o,\,\eta_o} \Delta\eta = e^{+\alpha^+ l}\, e^{-j\phi} \quad . \quad (10)$$

Thus, for a complete solution one needs to know the values of Pierce's parameters for the case $1/G = 0$. Assuming these values are known for the BWO, the following solution results:

$$\Delta b = \rho\ |H|\ \sin(A-\theta) \quad (11)$$

$$\Delta\eta = \zeta\ |H|\ \sin(G-B) \quad ,$$

where ρ, ζ, A, and B are functions of the backward-wave oscillator. Pierce's parameter b is now expressed as:

$$b = b_o + \Delta b \quad . \quad (12)$$

Voltage Tuning Curve

The voltage tuning for a backward-wave oscillator without a feedback circuit is given as:

$$\beta_e = \beta_{-1}\,(1 - Cb) \quad (13)$$

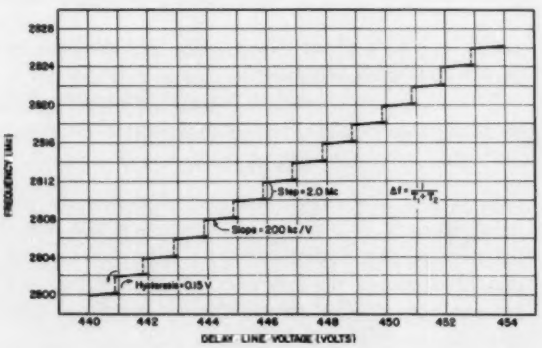

Figure 5.
Staircase tuning curve for QKB 924 BWO

and

$$V_o = \frac{m}{2e}\, u_o^2 = \frac{m}{2e}\, v_{-1}^2\,(1 + Cb)^2 \quad , \quad (14)$$

where u_o is dc beam velocity, V_o dc beam voltage, and v_{-1} phase velocity of -1 space harmonic. For the case of a backward-wave oscillator with an external feedback, the voltage tuning curve is written as:

$$V_o = \left(\frac{m}{2e}\right) v_{-1}^2 [1 + C\,\{b_o + |H|\,\rho \sin(A - \theta)\}] \quad . (15)$$

Hence the slope of the voltage tuning curve is $dV_o/d\omega$. For a backward-wave oscillator with feedback

$$\left(\frac{e}{2mV_o}\right)^{1/2} \frac{dV_o}{d\omega} = \frac{dv_{-1}}{d\omega}$$

$$[1 + C\,\{b_o + |H|\,\rho \sin(A - \theta)\}] \quad (16)$$

$$+ v_{-1}\, C\left[\rho \frac{d|H|}{d\omega} \sin(A - \theta) - \rho|H| \cos(A - \theta)\, \frac{d\theta}{d\omega}\right].$$

Since the feedback amplitude is not a function of frequency, $\frac{d|H|}{d\omega} = 0$ and also $b_o C \ll 1$, then Equation 16 becomes

$$\left(\frac{e}{2mV_o}\right)^{1/2}\frac{dV_o}{d\omega} = \frac{dv_{-1}}{d\omega} - v_{-1}C_p|H|\cos(A-\theta)\frac{d\theta}{d\omega}, \quad (17)$$

where, for a non-dispersive external line

$$\frac{d\theta}{d\omega} = \frac{d(\beta_{-1}L_T)}{d\omega} + \frac{l}{v_{ext}}, \quad (18)$$

where L_T is the total length of backward-wave oscillator.

Stabilization

Stabilization S is defined as:

$$S = \frac{\left.\frac{dV_o}{d\omega}\right|_{\text{no feedback}}}{\left.\frac{dV_o}{d\omega}\right|_{\text{with feedback}}}. \quad (19)$$

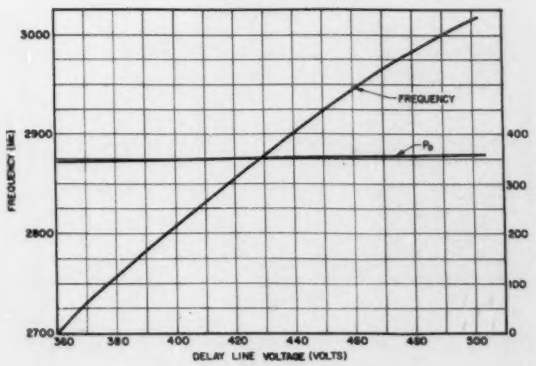

Figure 6.
Normal operating characteristics of QKB 924 BWO

This is obtained by differentiating Equation 14 and dividing by Equation 17. The result can be used to predict stabilization factors.

If the amplitude of the feedback is sufficiently large, there are only certain bands of frequency at which oscillation may occur (see the staircase tuning curve of Figure 5). The data presented are typical of those obtained over the entire frequency range of interest; i.e., 2700-3000 Mc. Although not shown, power output of the order of 20 milliwatts or more was obtained at the several frequency steps checked. This is more power than needed to saturate a low power traveling-wave tube amplifier, but appreciably less than that obtainable when operated as a normal backward-wave oscillator.

The hysteresis effect noted in the stepped tuning curve and which is repeatable, is advantageous to the equipment designer. It permits an additional 150 millivolts drift in the power supply when returning to a particular step without falling off that step as well as prevents unstable operation between steps.

Figure 6 represents the normal tuning curve of this backward-wave oscillator when it is terminated by a matched load, thus showing that the tube can be operated as a conventional BWO or with a feedback loop to get the stepped tuning curve. Again, it is pointed out that the data presented are limited to the frequency range of interest which is only one-sixth of the tube capability.

The frequency spacing between steps is found to be dependent upon the electrical length of the feedback loop and agrees with the relation that

$$\Delta f = \frac{1}{\tau_{BWO} + \tau_{ext}},$$

where Δf is in megacycles per second, τ_{BWO} is the wave transit time along the BWO, and τ_{ext} is the wave transit time along the transmission line. In terms of tube parameters, this becomes

TABLE I

DELAY LINE (feet)	FREQUENCY INCREMENTS (Mc)
50	10.2
100	8.5
200	4.5
300	3.0
400	2.0

$$\Delta f = \frac{1}{\frac{n[\omega(L+h) - \pi c]}{c\omega} + \frac{l}{v_{ext}}},$$

where n is the number of cells in the slow wave structure (interdigital line), c is the velocity of light, h is the finger length (interdigital line), L is the structure period (or pitch), ω is in radians per second, l is the length of external line, and v_{ext} is the phase velocity of wave in external line.

In practice, the external delay line is made many times longer electrically than the BWO, so that $\tau_{BWO} \ll \tau_{ext}$. Therefore, one can write that

$$\Delta f = \frac{1}{\tau_{ext}} = \frac{1}{l/v_{ext}} = \frac{v_{ext}}{l}.$$

The frequency increments between steps for various lengths of external delay lines are presented in Table I.

It is obvious then that for a given type of line the spacing between steps is essentially inversely proportional to the line length and directly proportional to the phase velocity of the rf wave in that line. At first glance, it appears that one may arbitrarily select any frequency separation between steps by the simple

expediency of changing the external line length. However, certain limitations become quickly obvious; if the line length is excessively long, then the attenuation becomes large enough so that a negligible amount of power is available at the input side of the slow-wave structure and the stepped tuning curve is not realized; and if the line is too short, then the stabilization factor is unsatisfactorily low even with relatively high feedback power levels.

A factor of S = 10 has been measured with a feedback loop consisting of 400 feet of 5/8 inch diameter styroflex coaxial line as shown in Figure 7. This figure presents stabilization factors versus feedback power for three different lengths of external feedback loop—in this case a 50-ohm styroflex coaxial line. The same stabilization factors are obtainable for different external line lengths provided the feedback power is increased as the line length is decreased. For a constant value of feedback power, stabilization increases with increasing line length or may not be attainable at shorter line lengths. For a given line length, a stability limit is reached at some feedback power level, and increasing the power feedback beyond this value no longer increases stability.

Stabilization versus frequency for a given line length is another item of interest. Figure 8 shows the stabilization factor obtained for a line length of 400 feet. The slope of the stabilization factor increases with increasing frequency. This is to be expected since the feedback power also is increased and it was previously established that stabilization does increase as the level of feedback power is raised.

So far, it has been shown that stability in terms of a reduction of tuning rate can be achieved by employing feedback with a backward-wave oscillator with the resulting tuning curve having a staircase appearance.

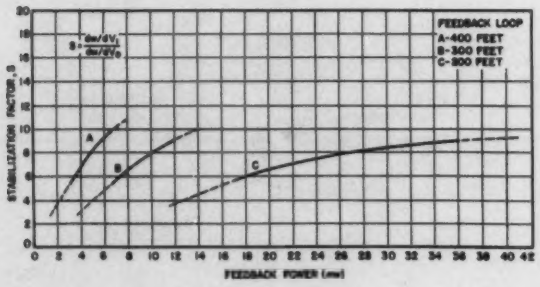

Figure 7.
Stabilization factor vs. power feedback for QKB 924 BWO

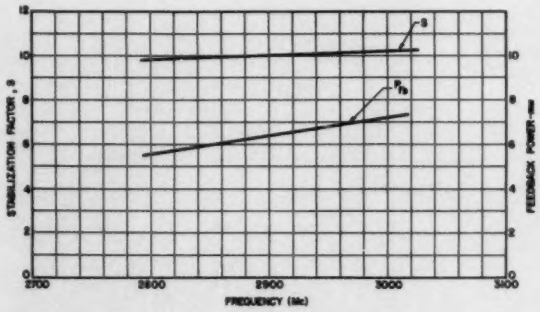

Figure 8. Stabilization factor and feedback power vs. frequency for QKB 924 BWO

TABLE II

FREQUENCY (Mc)	ANODE SENSITIVITY Δf/ ΔVa (anode) WITH FEEDBACK (Mc/volt)	ANODE SENSITIVITY Δf/ ΔVa (anode) WITHOUT FEEDBACK (Mc/volt)	GRID MODULATION SENSITIVITY Δf/ Δ Va (grid) WITH FEEDBACK (Mc/volt)	GRID MODULATION SENSITIVITY Δf/ Δ Va (grid) WITHOUT FEEDBACK (Mc/volt)
2500	0.05	0.59	0.15	1.75
2600	0.043	0.80	0.17	1.70
2700	0.06	0.44	0.14	1.20
2800	0.04	0.35	0.17	1.25
2900	0.06	0.52	0.23	1.75
3000	0.06	0.53	0.21	1.70
3100	0.06	0.45	0.29	1.50
3200	0.05	0.40	0.18	1.10

The frequency stability of oscillation at several of the steps in the 2700-3000 Mc range, was measured by H. G. Pascalar[4] of Lincoln Laboratory, Lexington, Massachusetts, by observing the beat frequency between the BWO and an S-band triode stalo. The test was performed by varying the beam voltage slowly until the frequency jumped (i.e., from one step to another) at which time the voltage was left fixed. The triode stalo was then tuned to obtain a one to ten kc per second beat frequency. The short term stability (peak to peak frequency deviation) measured was 200 cycles per second. The measured deviation was attributed mostly to 60 cycle and 120 cycle ripples in the power supply. The long term stability was checked over a period of one hour and the frequency deviation was less than 10 kc per second.

In addition to the items discussed above, the effects of feedback upon the grid and anode modulation sensitivity were also investigated. Table II compares the grid and anode modulation sensitivity for the two conditions with feedback and without feedback. The

[4]H. G. Pascalar, "An Investigation of Frequency Stabilization Techniques for Backward-Wave Oscillators," Lincoln Laboratory Report No. 48.7 (August 3, 1959).

data were taken at several oscillation frequencies of the BWO using a feedback loop of 300 feet of coaxial cable.

The decrease in modulation sensitivity of both the grid and anode of the BWO is comparable to the stabilization factor with minor deviations probably due to measurement error.

The effects of feedback upon the frequency modulation of the signal because of the use of an ac heater supply were also determined. As a comparison, data were taken with and without feedback; in both cases, a 60 cycle ac heater supply was used. The results are shown graphically in Figure 9 where a substantial reduction in signal frequency modulation is noted. For some applications, this residual FM may be permissible,

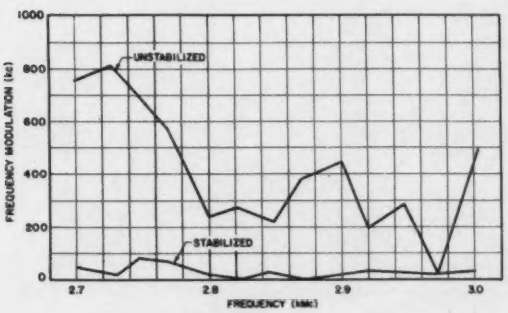

Figure 9. Heater frequency modulation vs. frequency for QKB 924 BWO

but for optimum signal stability, the use of a dc filament supply is necessary.

Employing feedback has also produced other effects. The BWO tested had a spurious oscillation amplitude 45 db below and within one megacycle of that of the main signal when operated as a normal BWO. However, with feedback, the amplitude of the spurious signal was further reduced by 15 db to a level 60 db below that of the main signal. This result was consistent over the range of the tube tested, i.e., 2700-3000 Mc, and it is assumed that similar results would occur outside of this frequency range.

The effect of ambient temperature variations upon the frequency of oscillation of the BWO was also determined.

In the first experiment, the tube was run as a conventional BWO and the ambient temperature varied from 0° to 65° C. The net frequency drift recorded was 2.4 Mc. A 200-foot length of ⅝ inch diameter styroflex coaxial cable was then connected to the tube as the external circuit. The external circuit was maintained at room temperature while the tube was again cycled in an ambient temperature change of 0° to 65°C. The frequency drift recorded was now down to 0.27 Mc.

In the next experiment both the tube and external circuit were subject to ambient temperature changes from 0° to 65°C. The frequency drift recorded was 0.8 Mc. Frequency drift of the composite system, BWO plus the external loop, due to changes in ambient temperature is one-third that observed on a conventional BWO.

Conclusion

It has been shown that a BWO modified so that part of its output is fed back through a long external loop has certain desirable characteristics. Oscillations occur only at discrete frequencies as the beam voltage is varied. In addition, frequency of oscillation is very stable. This device (BWO plus feedback loop) is well suited for applications such as frequency-diversity radar where rapid switching over a large frequency band may be required.

From the analysis, a successful backward-wave oscillator with an external circuit depends upon:

1. High gain backward-wave oscillator,
2. Input and output of backward-wave oscillator well matched to external line,
3. External delay line with low attenuation.

The principal characteristics of a stabilized backward-wave oscillator are:

a. *Oscillation*

$GHf = 1$

G = gain of backward-wave oscillator

H = $e^{-\alpha+l}$ attenuation of the external line

f = fraction of output power feedback from backward-wave oscillator to sustain oscillation.

b. *Stabilization*

Stabilization is directly proportional to the length of the external line and amount of the feedback power, while indirectly proportional to attenuation and the phase velocity of the external line.

c. *Frequency Steps*

The frequency steps are inversely related to the length of delay line of the backward-wave oscillator and external feedback loop, while directly proportional to their phase velocities.

While a complete analysis of a composite system of the backward-wave oscillator with an external feedback loop is difficult, the important characteristics can be determined from the parameters of the external line. Coupling the values of external line parameters with experimental data will give the necessary information for the design and operation of this type of device.

The Raytheon S-band BWO with permanent magnet focusing is well suited for the device described in this paper since its electrical input requirements can be readily met by precision-regulated power supplies. Thus, one avoids the complex electronic stabilizing circuitry that would otherwise be needed if this type of device were not employed. ■

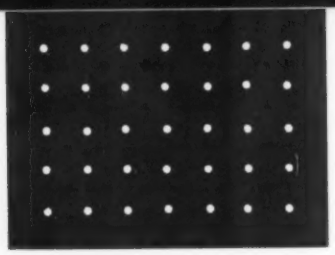

by WALTER A. DOESSCHATE, JR.

A DESIGN TECHNIQUE FOR HIGH SPEED TRANSISTOR CIRCUITS

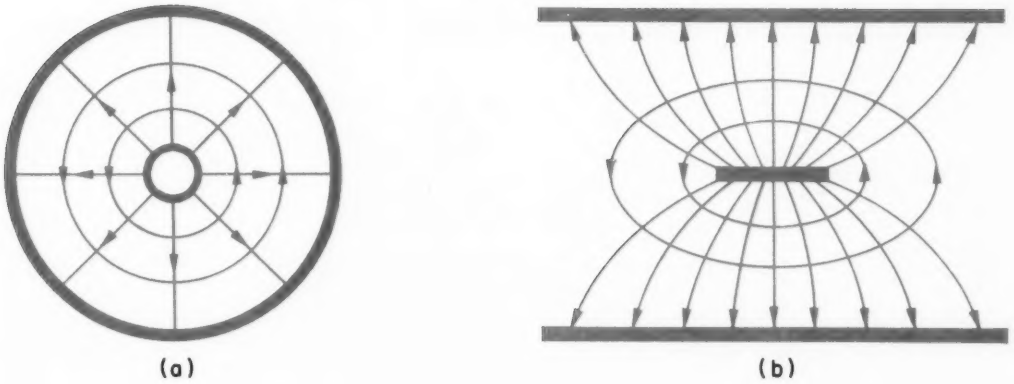

Figure 1. The difference between (a) coaxial transmission line and (b) strip transmission line. (Note the absence of the electric field at the sides)

WITHIN the past year the switching speed of transistors has increased so much that conventional methods of circuit layout are practically useless. Unusual waveforms are often observed when the rise time of the applied pulses is in the order of nanoseconds. Delays, ringing, and over-all unpredictable wave shapes occur in even such simple circuits as inverters. These phenomena can usually be attributed to either the circuit layout, component inadequacy, or both. This paper will concern itself only with circuit construction. A new method of breadboard construction as well as a discussion of other successful methods of circuit arrangement will be considered in this article.

Since much work has been done with high frequencies using coaxial air lines manufactured by General Radio (type 874), it was natural to apply this method to circuitry involving fast rise and fall pulses. For the most part excellent results have been obtained; however, even with these good results the coaxial transmission line method has a considerable number of drawbacks.

Cost and complexity are the most important items of concern regarding any system. Many of the parts of the air coaxial line system must be precision machined which keeps the price of the component parts rather high. The complexity of the system is evident to anyone who has ever seen even simple circuits laid out using these techniques. There are also the problems of conforming the pipe diameter to accommodate the small diameter of the transistor lead without destroying the usefulness of the system and the requirement that each end of the line must be matched so that serious reflections, attenuations and delays will not result. For these reasons a system of strip transmission line was developed.

The strip transmission line system consists basically of two flat conducting plates precisely spaced with a flat center conductor running down the center between the two plates. Figure 1 shows the transition from coaxial line to the strip line and how the electric and magnetic fields are concentrated. This system now allows the insertion of lumped parameters through the side openings without the interference of the electric field since it is concentrated more or less vertically. Strip transmission line is more compact and transistor sockets may be used; however, coaxial transmission lines must be used as connections between the strip line and associated equipment.

The construction of a multivibrator, for example, in either strip line or coaxial line involves a good deal of money and time. Parts for either system are not always available and the work of actual construction must be done by an experienced person. The problem of changing a capacitor or a resistor value in either system requires a major operation and a trial and error method of speed-up capacitor selection, for example, is very time-consuming and expensive.

A comparison of results from standard wire and solder techniques and strip line methods seems to indicate a method of construction which would fit in the frequency range between these two systems. The high frequency systems are absolutely necessary but are not required by most of the transistor field as yet. We then developed another system of breadboarding which is cheap, quick, easy to construct, and provides excellent results. A specially skilled person is not needed for construction and the parts required are easy to obtain.

This system of preliminary circuit construction revolves about the use of a copper laminated board for both ground and mounting. Components are soldered directly to ground and mounting of parts is done by soldering them to the ground plane directly. Arrange-

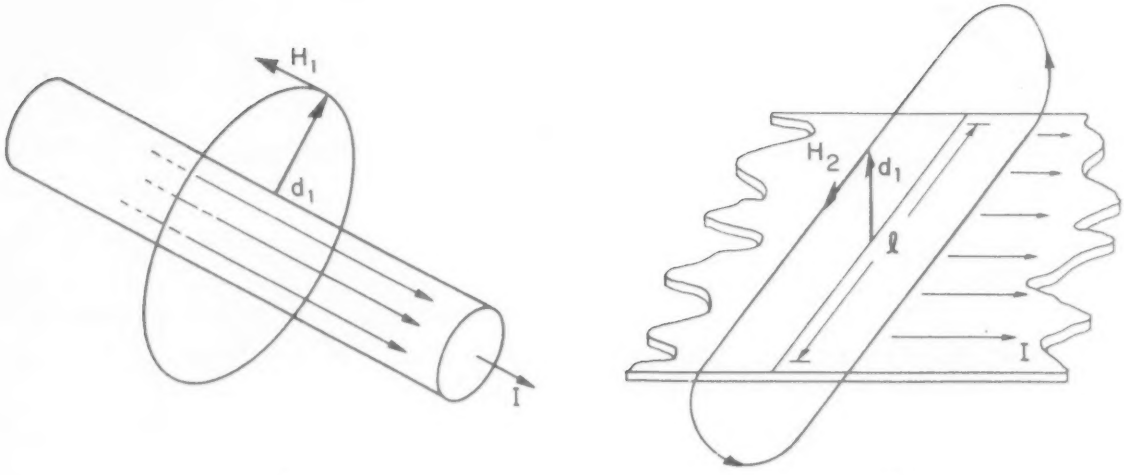

Figure 2.
The magnetic field about (a) the wire and (b) the conducting plane

ment is not limited to the right angle layouts to which one is usually restricted with circuit board. The parts used in construction may be used over and over again.

The reason for using a copper laminated board results from the theory involving an infinite plane of conducting material. If a conductor having a circular cross section with a current (I) flowing through it is considered, then a magnetic field will exist as shown in Figure 2a. The field surrounding the wire may be calculated using Maxwell's first law which is $I = \phi Hxdl$. Then at a certain distance d_1 from the conductor the field strength may be found to be a value H_1. If we compare this case to the case shown in Figure 2b where a large but finite plane of conducting material of length l with a sheet current of magnitude I flowing in it, we would find that at the same distance d_1 from the surface a magnetic field of H_2 is found. Since the length of the path which the field must follow has increased, $H_2 < H_1$. As the length of the plane perpendicular to the sheet current is increased, the field strength at d_1 decreases and as a limiting case H at d_1; goes to zero as l goes to infinity.

This of course is an ideal case since no sheet current would exist as such in a normally constructed circuit. Figure 3 shows the more practical case and how the field would vary about the surface of the copper clad sheet if a current I was to flow from point a to b. The field would not be constant at any given distance from the surface but would also vary with the distance from the current flow center due to the probable symmetry of current flow about the center line a, b as shown. It can be seen however that the field is still much more concentrated near the copper clad board than it is in the case of the circular cross section conductor. The copper clad board greatly reduces the inductive properties of the ground section of the circuit and thus improves over-all circuit performance.

Two other factors which limit normal breadboard construction are skin effect and the restriction of current flow in the ground plane. At high frequencies currents tend to flow on the surface of the wire and the larger the surface the lower the high frequency resistance. A ground plane as described here has a large surface area and thus negligible resistance at extremely high frequencies. The current restriction mentioned refers to the fact that currents can only flow in either of two directions in a wire. This coupled with the high resistance produced by the skin effect causes the addition and subtraction of ground currents. This can cause a great deal of trouble when they become involved in the base circuit of a transistor where they can be amplified. With a ground plane, currents can flow in any direction whatever and interaction is at a minimum. This conglomeration of waveforms in the ground lead of a conventionally breadboarded circuit can actually be observed on a scope by placing the ground lead of a scope to one end of the circuit ground line and traveling along the ground line with the probe. The use of the copper laminated board coupled with a few adaptations of normal procedures has provided excellent results.

The parts required for construction are extremely cheap and easy to obtain. The copper clad laminated board may be obtained at any electronic supply house. The other parts used consist of Alden circuit board cut into strips which have one series of holes down the center, Alden board lugs, standoffs, and conch type

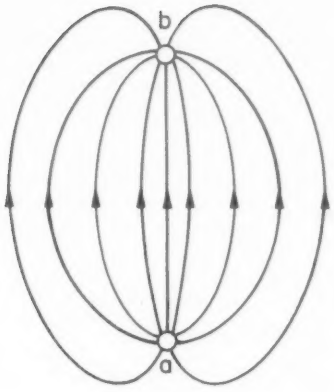

Figure 3a.
Top view of copper plate showing current flow

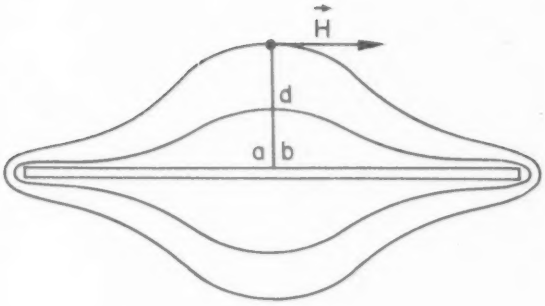

Figure 3b.
Side view of copper plate showing associated field

transistor sockets. A few nuts and bolts and solder lugs are also required.

A few words should be said about the transistor socket used. (See Figure 4.) Most circuits after they are breadboarded require interchangeability tests and this requires clipping of the leads of many transistors to cut down lead inductance. By drilling a hole in the rear of the socket at the center of the slit through which the spring clip lug extends a transistor with long leads may be inserted into the socket and the leads pulled out the other side where the lug sticks out. This allows the socket to grab the transistor at the base of the leads and as long as the leads are kept away from the other parts of the circuit they have no effect on the circuit operation. The socket may be soldered to the board via a solder lug and a nut and bolt.

The Alden board clips and the circuit board strips comprise the system by which the components are mounted. The strips are mounted to the board by inserting standoffs in strategic positions along the board and then soldering the other end of the standoff to the board. This arrangement is shown in Figure 5b where a Nand gate has been constructed. Soldering to a laminated copper board is relatively easy since the copper is very thin and heats up without any difficulty using a standard soldering iron. Generally all the hardware required in normal circuitry can be mounted using solder lugs or soldering directly. If a more solid or permanent connection is required the holes may be drilled easily and the part simply bolted on.

To provide a comparison of the copper clad method of breadboarding with the strip line techniques, two circuits were chosen. The first was a Nand gate which incorporated Raytheon's 2N828 epitaxial mesa. (See schematic in Figure 6.) Figures 5a and b show the two methods of breadboard layout used. Standard parts were used in both circuits and the same transistor was used in both tests. Figure 7 shows the results obtained.

By comparing the resulting wave forms, it can be seen that except for the ringing in Figure 7a—the standard layout—the wave shapes are almost identical. Closer inspection brings to view a slightly faster rise time in the standard breadboard circuit. This is a direct result of the ringing since somewhere in the

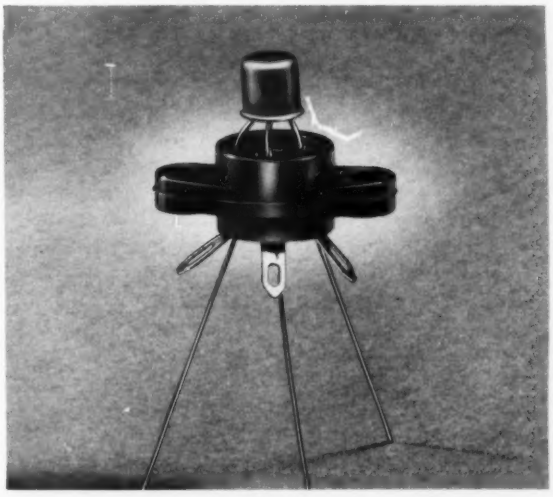

Figure 4.
Modified transistor socket with transistor inserted

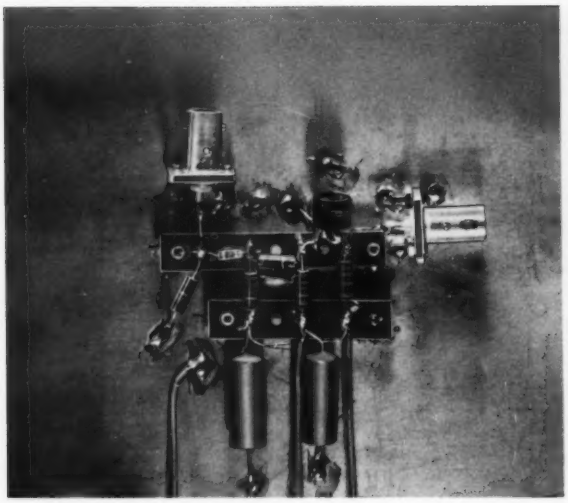

Figure 5a. Copper clad method of breadboarding

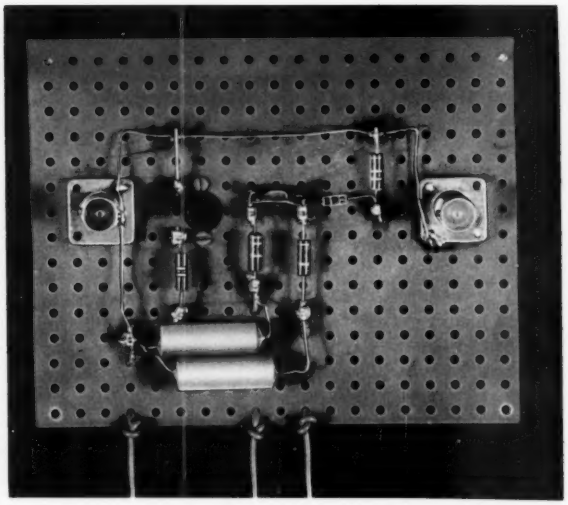

Figure 5b. Strip line method of breadboarding

layout there is one or more stray damped tank circuits. This is the circuit property which gives a slightly faster rise time but also provides the ringing component viewed in the waveform. The slight difference in rise time is not capacity to ground in the copper clad layout because that effect would certainly be evident in the fall time and the fall times of both circuits are almost identical.

To prove that the copper clad method is truly a transition method between standard breadboard layouts and high frequency techniques a second comparison was made using an avalanche transistor pulse generator employing one of Raytheon's 2N1468 avalanche transistors. The same circuit, shown in Figure 8, was laid out in strip line, the copper clad board method, and in standard breadboarding. The results obtained through this comparison appear in the waveforms of Figure 9a, b, c, and d.

Figure 9a, the standard breadboard technique, shows a definite decrease in the rise time as compared with Figure 9b, the copper clad board method. This difference is definitely a property of the circuit layout since standard components were used in both circuits and the same transistor was also used in all three circuits. Figure 9c shows the same waveform obtained in strip line and it appears that there is only a slight increase in the rise time when Figure 9b and c are compared. The entire output waveform is shown in Figure 9d.

The results obtained definitely indicate that the copper clad board method of construction outlined here is a transition system between the standard breadboard methods and the high frequency techniques. Another result is that the copper clad board method may be used to lay out a circuit to check its operation and component choice previous to its construction in strip line or coaxial line layouts. This would tend to be a definite time-saving technique. It should also be noted that the only transistors which require the high frequency techniques are the avalanche transistors since their switching speed is less than a nanosecond.

The cost, ease of construction, and electrical results definitely indicate the advantages of this type of construction over all other methods for the types of high speed and high frequency transistors now on the market. Excellent results were obtained in all cases and no rearrangement of components was required in any case. ■

WALTER DOESSCHATE, JR. *is an Applications Engineer at the Silicon Operation, Semiconductor Division. Since joining Raytheon in 1960, he has worked on high speed switching circuitry involving the epitaxial mesa transistor. Mr. Doesschate received a B.E.E. degree from Brooklyn Polytechnic Institute in 1960.*

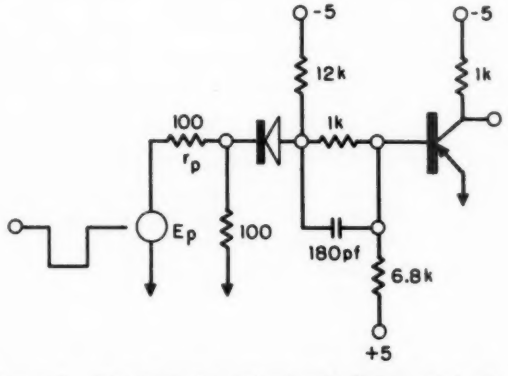

Figure 6. Circuit used as Nand gate (with outputs shown in Figure 7 and construction in Figure 5)

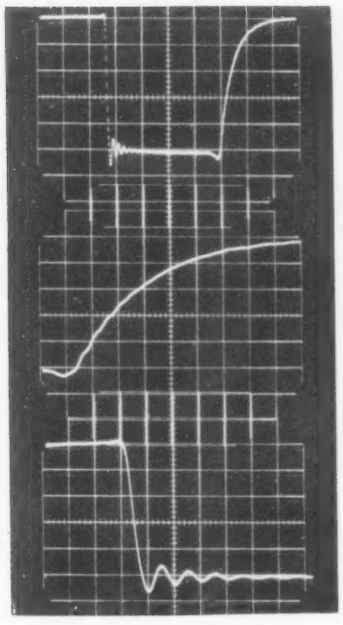

Figure 7a.
Nand gate of standard construction showing output waveform (25 ns/cm), fall (5 ns/cm), and rise (5 ns/cm)

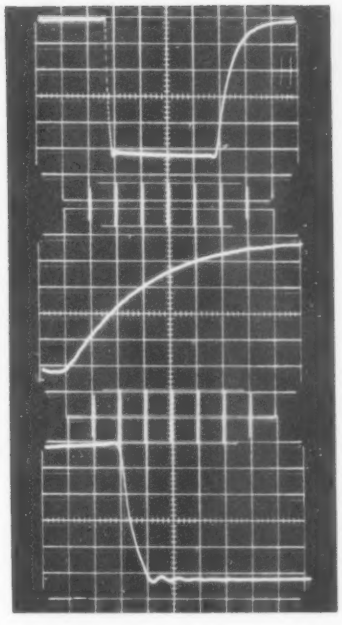

Figure 7b.
Copper clad construction of Nand gate showing output (25 ns/cm) fall (5 ns/cm), and rise (5 ns/cm)

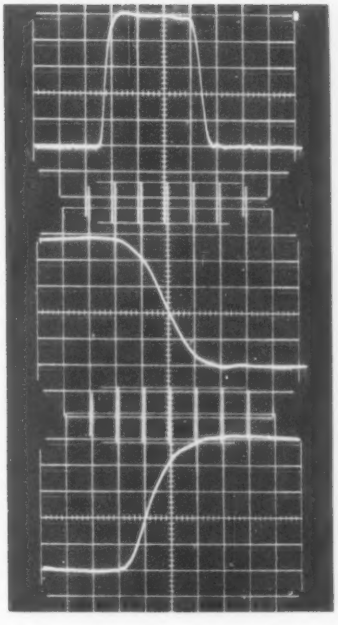

Figure 7c.
Input waveshape to Nand gate (25 ns/cm), fall (5 ns/cm), and rise (5 ns/cm)

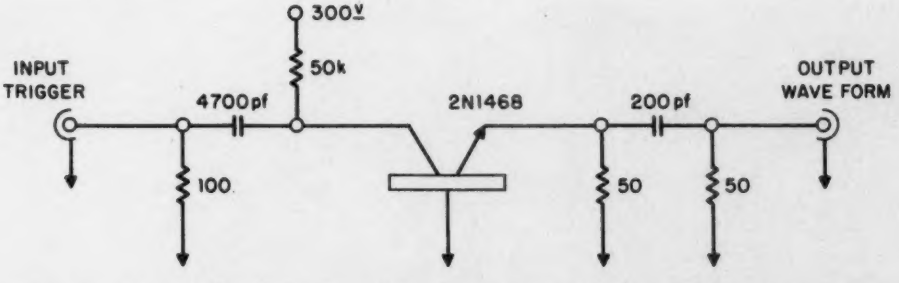

Figure 8. Avalanche pulse generator with external trigger input using the 2N1468

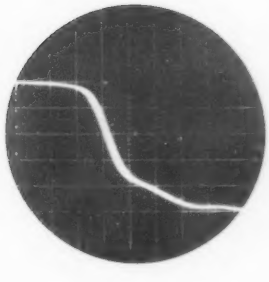

Figure 9a.
Standard circuit arrangement at 1 ns/cm

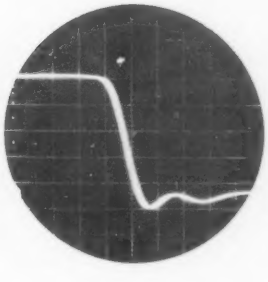

Figure 9b.
Copper clad layout at 1 ns/cm

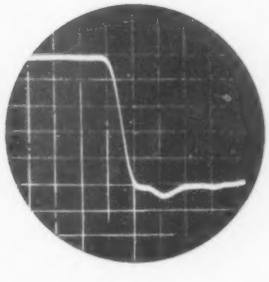

Figure 9c.
Strip line procedure at 1 ns/cm

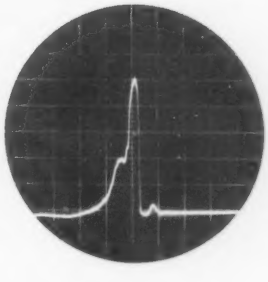

Figure 9d.
Output waveshape at 25 ns/cm

Figure 9. Comparison of output waveshapes between the three different types of circuit layout

PRINCIPLES OF

ASTRONAUTICS 3

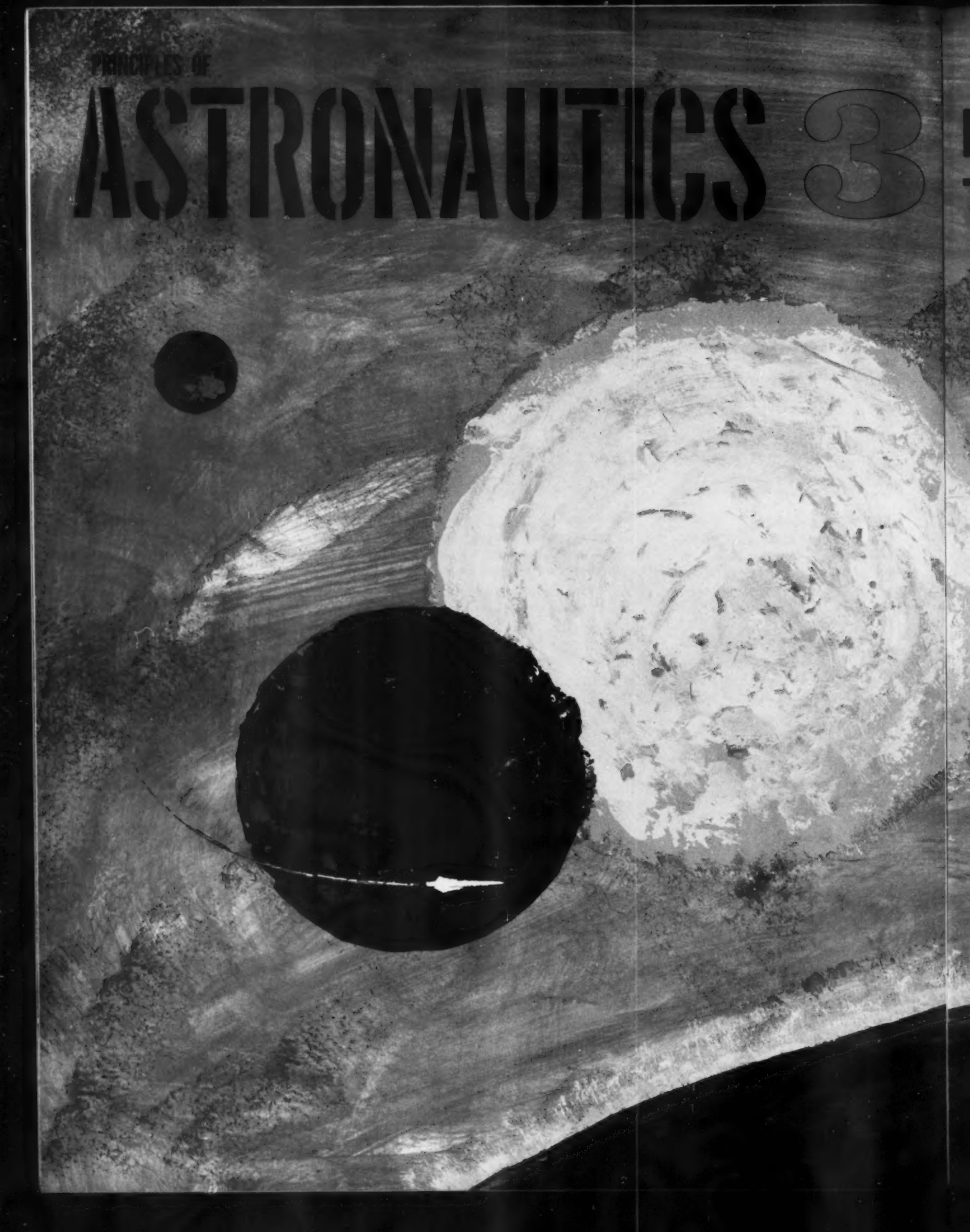

INTERPLANETARY TRANSFER

by Gerald A. Ouellette

THE desire to visit the planets has persisted since the time it was first recognized that the planets are not wandering stars, but satellites of the Sun. Scientists postulated that life forms could exist on these planets and science fiction writers used this as a basis for some rather fanciful conjectures as to the extent of intelligent life in the solar system. It was perhaps a logical extension of these conjectures that imaginary journeys of spacemen to the planets have dotted the literature for centuries. Technological advancements, however, have indicated that even a small expedition to the near planets would tax the economy as well as the technology of the great nations of the Earth. Despite the magnitude of the required effort, interplanetary flight will, in all probability, be attempted during the next few decades as a logical extension to current space programs.

The requirements for interplanetary flight differ from those for lunar operations primarily in the length of time over which the vehicle system must remain operable and in the increased performance capability of the propulsion system. The longer flight times, on the order of two to three years in contrast to several days for lunar round trips, pose serious problems for manned flight, especially in the areas of long term exposure to radiation, emergency rescue capability, and psychological and physiological effects of isolation in an unnatural environment. Since human factors do not affect the mission performance requirements, performance can be discussed parametrically without recourse to problems associated with manned flight.

The requirements for any space mission can be expressed in terms of a characteristic velocity, which, independent of the vehicle configuration, is used as the basic parameter in determining mission criteria. In general, interplanetary flight can be separated into three relatively distinct phases: 1) escape from the parent planet, 2) motion along a heliocentric (Sun-centered) orbit that intersects the solar orbits of the two planets, and 3) capture and planetfall at the target planet. The conditions in terms of position and velocity at the end of one phase must satisfy the initial conditions of the succeeding phase. The requirements for accomplishing each of these phases will be discussed along with an approximate discussion of end-point matching between the various phases of flight.

Planetary Escape

In 1609 Johannes Kepler published his proof, based on Tycho Brahe's observational data, that the planets

move in elliptical orbits about the Sun. Sir Isaac Newton, in 1687, published the results of his work on gravitation which generalized Kepler's results for celestial motion by proving analytically that the motion of a body acted upon by any central gravitational field will trace out a conic section. The conics along which motion is possible are the ellipse, the parabola, and the hyperbola, with the circle as a limiting ellipse and the straight line as a limit in all cases. The period of motion along the parabola and hyperbola is infinite; therefore, if a space vehicle can be injected into such an orbit it will move away from the attracting center indefinitely. Planetary escape is thus accomplished by accelerating a spacecraft to a velocity so that it satisfies the requirements for motion along either of these two types of conics. Since the parabola represents the infinitesimal dividing line between the ellipse and hyperbola, parabolic motion is not practical in the real sense.

The type of orbit traced out by a body under the influence of a central force can be determined from its total energy, which is a function only of the magnitudes of its velocity and radius vectors relative to the attracting center. The total specific energy can be expressed as the sum of the kinetic and potential energy of the orbiting body.

$$E = KE + PE = \frac{1}{2} v^2 - \frac{\mu^2}{r} \quad , \quad (1)$$

where v, r, and μ^2 are the velocity, radius, and gravitational constants, respectively. The zero point for the potential energy in Equation 1 is at infinity. It is apparent from this equation that the relations in Table I hold.

When the energy equation satisfies the relation $E \geq 0$, reaction thrust is terminated and the subsequent motion is along an escape orbit. The powered motion of the trajectory is similar to that followed by a satellite launching vehicle although the burning time is considerably longer since the burnout velocity is approximately half again that required for establishing a satellite orbit.

The well-known equation for escape velocity ($v_{e\oplus}$) at the Earth's surface ($r = r_o$) is obtained from Equation 1 by setting $v = 0$ at $r = \infty$, and using this to find $v_{e\oplus}$ when $r = r_o$, i.e., setting $E = 0$ and solving for v_e. Thus,

$$v_{e\oplus} = \sqrt{2 g_o r_o} \quad , \quad (2)$$

where g_o is the gravitational acceleration at the Earth's surface and $g_o r_o^2 = \mu^2$ by definition. Escape velocity at any radius from the geocenter (Earth center) can be obtained by combining Equations 1 and 2, which in general gives

$$v_e = v_{e\oplus} \sqrt{r_o / r} \quad . \quad (3)$$

The above equations hold for any celestial body and values of the constants for the planets and the Sun and Moon are given in Table II.

TABLE I

ALLOWABLE MOTION IN AN INVERSE SQUARE GRAVITATIONAL FIELD

E	MOTION	r_{max}	$v(r_{max})$
<0	elliptic	finite	≥ 0
$=0$	parabolic	∞	0
>0	hyperbolic	∞	>0

A vehicle escaping from the Earth recedes along a hyperbola as shown in Figure 1. For practical purposes the vehicle is considered to have reached infinity with respect to the Earth when $r/r_o > \sim 250$, and subsequent motion is under the influence of solar gravity. In general, the vehicle will possess a velocity at infinity called its hyperbolic excess velocity which is determined by Equation 1. Thus, for some initial conditions (taken at thrust termination or cutoff), v_{co}, r_{co}, and for $r \gg \mu^2$, the hyperbolic excess velocity is

$$v_\infty = \sqrt{v_{co}^2 - v_e^2} \quad . \quad (4)$$

The vector sum of the hyperbolic excess relative to the Earth and the Earth's orbital velocity relative to the Sun expresses the vehicle velocity relative to the Sun. This velocity and the vehicle position vector are used to determine the subsequent motion relative to the Sun, i.e., its heliocentric orbit. Some error is introduced by this simplification, but it is insignificant in a mission criteria study.

When large space vehicles are needed, it may be impossible to launch them directly from the surface of the Earth, thus necessitating assembling the vehicle in a circular satellite orbit. Escape from this type of orbit is accomplished by incrementing the orbital velocity by the difference between the orbital velocity and the cutoff velocity, v_{co}, that gives the desired hyperbolic excess. Since orbital velocity can be expressed as

$$v_s = v_e / \sqrt{2} = \mu / \sqrt{r} \quad , \quad (5)$$

the characteristic velocity for escape is given by

$$v_c = \sqrt{v_e^2 + v_\infty^2} - v_s \quad , \quad (6)$$

where $v_{co} = v_s + v_c$. The resultant motion is similar to that of the direct ascent in Figure 1, which illustrates a departure from the Earth for transfer to an outer planet.

Transfer Orbits

As initially proved by Kepler, the planets move in elliptical orbits about the Sun; however, since these orbits have very small eccentricities, they can be considered circular for study purposes, without introducing excessive error into the analysis. The orbital planes of the planets also have only small inclinations relative to the Earth's orbital plane. Assuming these angles are zero, all motion can be considered coplanar, again

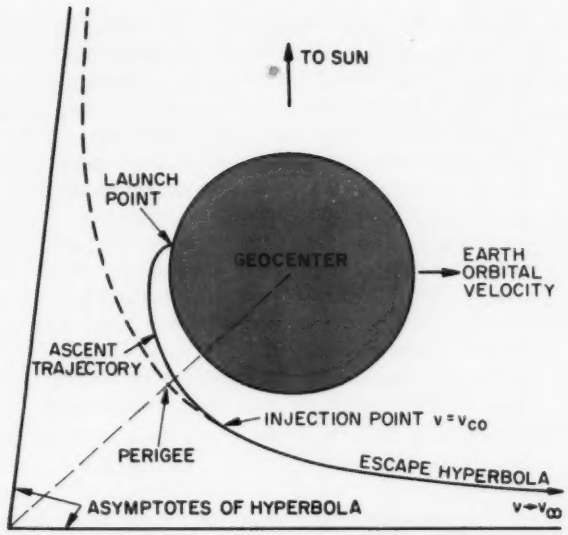

Figure 1a. Direct ascent hyperbolic escape orbit

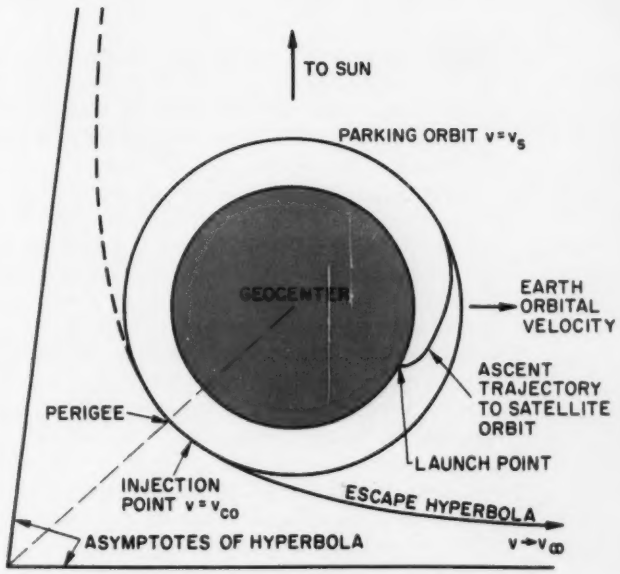

Figure 1b. Indirect ascent hyperbolic escape orbit

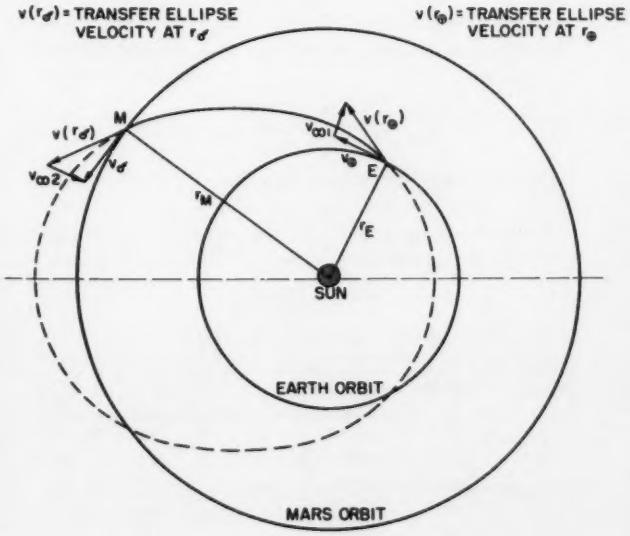

Figure 2. General elliptic transfer orbit between coplanar circular orbits

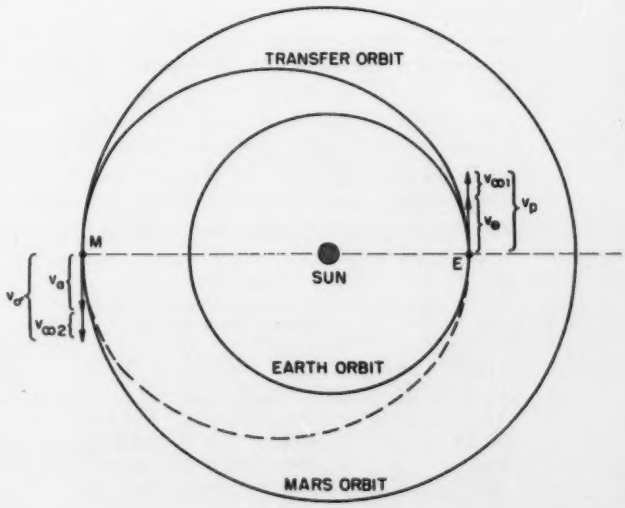

Figure 3. Cotangential (Höhmann) transfer orbit between Earth and Mars

introducing little error. An exact analysis would, of course, preclude such simplification since even small errors produce large secular deviations with time along an orbit. Some orbital parameters of interest for the solar system are presented in Table III.

Using the above model, interplanetary transfer is accomplished by injecting the space vehicle into a heliocentric orbit that intersects both the orbit of the Earth and the target planet. The conditions at injection are satisfied by the velocity and position vectors of the vehicle after it has escaped from the Earth, i.e., after it has approached sufficiently close to the asymptote of the escape hyperbola to neglect the effects of the Earth. (See Figure 1.) The type of orbit can be determined by using Table I and the vehicle's total energy relative to the Sun as given by Equation 1 with the solar value of μ^2. Because of the large amount of propellant required to accelerate the space vehicle to its final velocity, orbits requiring a minimum amount of energy, i.e., smallest possible v_∞ are desirable, thus, for practical purposes, interplanetary transfer orbits will, in general, be ellipses. Figure 2 illustrates the geometry showing the velocity vectors necessary to effect the transfer between the Earth and Mars. From this figure, it is apparent that two discrete velocity changes are necessary, one at E to enter the transfer ellipse, and one at M to exit from it. In some cases, the second velocity increment may be avoided if atmospheric braking techniques are used at the target planet to provide the necessary energy change. This technique will be discussed in more detail in a forthcoming paper of this series.

In 1924 Höhmann showed that the minimum energy two-impulse transfer orbit between two coplanar circular orbits is an ellipse tangent to the two orbits. (See Figure 3.) If the ratio of the two orbital radii exceeds approximately twelve, a three-impulse maneuver using two elliptical arcs requires less energy but this advantage is overshadowed by the extremely long transfer time which renders the maneuver impractical.

To effect the Earth-Mars transfer illustrated in Figure 3, a body in orbit at E in order to enter the transfer ellipse, must increment its velocity by the difference between its orbital velocity and the perihelion velocity of the transfer ellipse. Similarly, to exit from this ellipse at M it must again increment its velocity by the difference between orbital velocity at M and aphelion velocity of the transfer ellipse. Since the respective velocity vectors are colinear, the incremental velocities are also colinear, and thus tangent to the orbits at E and M. The hyperbolic excess velocity v_∞ is this exit velocity increment and its asymptote must be tangent to the orbit as shown in Figure 1.

The magnitude of the hyperbolic excess is determined from the vis-viva equation for the transfer ellipse

$$v = \mu\left(\frac{2}{r} - \frac{1}{a}\right)^{1/2} , \qquad (7)$$

by substituting in the respective values for a and r and by comparing the results at E and M. Since the transfer ellipse has its perihelion at E and aphelion at M, the semi-major axis is $a = (r_\oplus + r_\sigma)/2$, and the perihelion and aphelion velocities are

$$v_p = v_\oplus \sqrt{\frac{2K}{1+K}} \qquad (8)$$

and

$$v_a = v_\oplus \sqrt{\frac{2}{K(1+K)}} = v_\sigma \sqrt{\frac{2}{1+K}} , \qquad (9)$$

where $v_\oplus$ and v_σ are the Earth's and Mars' orbital velocities, respectively and $K = r_\sigma/r_\oplus$. The required hyperbolic excess to enter an Earth-Mars transfer orbit is therefore

$$v_{\infty 1} = v_\oplus \left(\sqrt{\frac{2K}{1+K}} - 1\right) \qquad (10)$$

and to exit from it at near Mars is

$$v_{\infty 2} = v_\sigma \left(1 - \sqrt{\frac{2}{1+K}}\right) . \qquad (11)$$

TABLE II

PHYSICAL CHARACTERISTICS OF BODIES IN THE SOLAR SYSTEM

BODY	ASTRONOMICAL SYMBOL	EQUATORIAL RADIUS (nautical miles)	SURFACE GRAVITY g_0 (ft/sec²)	GRAVITY CONSTANT μ^2 (ft³/sec²)	ESCAPE VELOCITY v_e (ft/sec)
Sun	☉	375,560		4.67898×10^{21}	
Mercury	☿	1,350	11.36	7.645392×10^{14}	13,654
Venus	♀	3,348	27.67	1.14499×10^{16}	33,553
Earth	⊕	3,440	32.25	1.407528×10^{16}	36,645
Moon	●	940	5.32	1.7270×10^{14}	7,873
Mars	♂	1,787	13.19	1.51520×10^{15}	16,705
Jupiter	♃	37,730	90.79	4.46723×10^{18}	624,260
Saturn	♄	31,075	41.81	1.33776×10^{18}	119,039
Uranus	♅	13,770	31.44	2.04599×10^{17}	69,937
Neptune	♆	13,500	36.83	2.42259×10^{17}	76,860
Pluto	♇	—	—	—	—

TABLE III

ORBITAL PARAMETER OF THE PLANETS

PLANET	MAJOR AXIS (a)* (Å)	ECCENTRICITY (e)	INCLINATION TO ECLIPTIC PLANE** 0	I	II	ORBITAL PERIOD (years)
☿	0.3871	0.20563	7	0	14.2	0.2411
♀	0.7233	0.00679	3	23	39.1	0.6156
⊕	1.0000	0.01673	0	0	0	1.0
♂	1.5237	0.09337	1	50	50.8	1.882
♃	5.2028	0.04843	1	18	19.9	11.86
♄	9.539	0.05569	2	29	42.2	29.46
♅	19.1820	0.04720	0	46	22.9	84.0
♆	30.0577	0.00857	1	46	26.5	164.8
♇	39.5177	0.24864	17	8	38.4	247.7

*r_σ = semi-major axis of Mars, etc.
Å = semi-major axis of Earth's orbit

**Ecliptic plane is Earth's orbital plane

The hyperbolic excess velocities required for a cotangential transfer between any two planets in the solar system are given in Table IV along with the idealized cutoff velocity required at the surface of the planet as given by Equation 4.

Equations 10 and 11 can be used to determine the characteristic velocity for simple interorbital transfer about any attracting center, for example, between two earth satellite orbits. In this case, the total velocity is

$$v_c = v_{s1}\left\{\left[\sqrt{\frac{2K}{1+K}} - 1\right] + \left[\frac{1}{\sqrt{K}} - \sqrt{\frac{2}{K(1+K)}}\right]\right\} \quad , \quad (12)$$

where K is the ratio of the outer (r_2) to inner (r_1) orbital radius, and $v_{s1} = \mu/\sqrt{r_1}$ is satellite velocity at r_1. It is interesting to note that this equation exhibits a maxima when the radius ratio is 15.58172. (See Figure 4.) Figure 4 shows dimensional values of the requirements for simple transfer between two Earth satellite orbits—the lower one having an orbital altitude of 110 nautical miles—and between the Earth's orbit and any other solar orbit. For intersatellite transfer, the maxima occurs when the higher orbital radius is approximately 55,000 nautical miles; for interorbital transfer for the Earth's orbit, the maxima occurs between Saturn and Uranus.

The relative positions of the planets must satisfy certain requirements when the transfer is initiated if the vehicle is to arrive at M coincidentally with the planet Mars. Since the transfer time is just the half period of the ellipse,

$$t = \frac{P}{2} = \frac{\pi a^{3/2}}{\mu} \quad . \quad (13)$$

During the time period t the radius vector of planet Mars sweeps through $t\omega_{\sigma'}$ degrees where the orbital angular rate $\omega_{\sigma'} = v_{\sigma'} / r_{\sigma'}$. The lead angle between the two planets at the start of the transfer is therefore

$$\psi = 180° - t\omega_{\sigma'} \quad . \quad (14)$$

Figure 5 illustrates the geometry for a round trip to Mars and indicates the length of time that the vehicle must remain near Mars until the lead angle is suitable for the return trip, in which case

$$\psi' = 180° - t\omega_{\oplus} \quad . \quad (15)$$

The transfer times for general interplanetary transfer are given in Table IV.

The results presented in Table IV give some indication of the extremely long transfer times for travel to the more distant planets using the Höhmann type transfer. Travel to the outer planets must therefore await the development of nuclear or nuclear-electric propulsion units capable of placing the vehicle in a high energy transfer orbit. The travel time to the outer planets

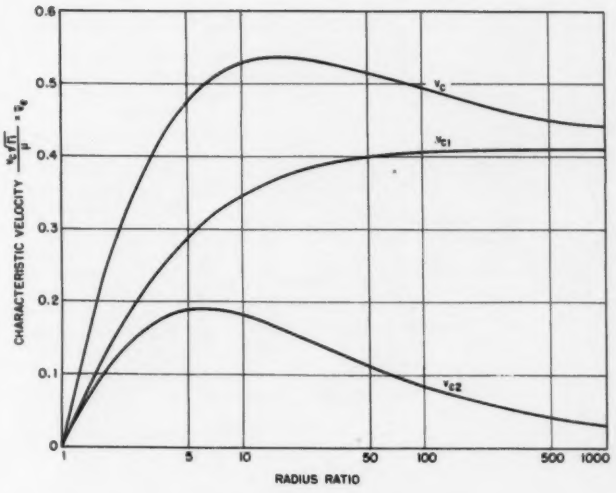

Figure 4a. Characteristic velocity for cotangential maneuver vs. radius ratio

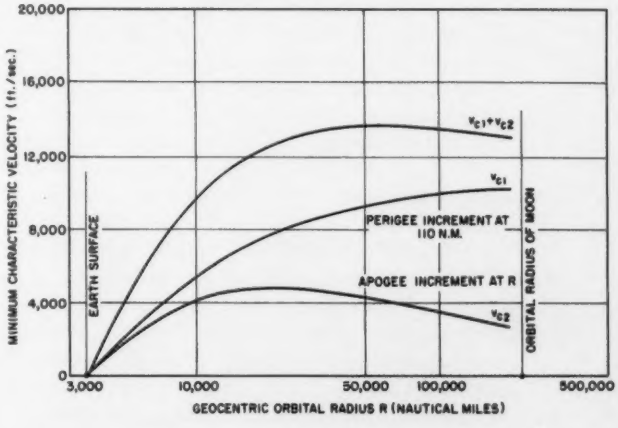

Figure 4b. Characteristic velocity required to increase orbital altitude from 110 nautical miles initial altitude

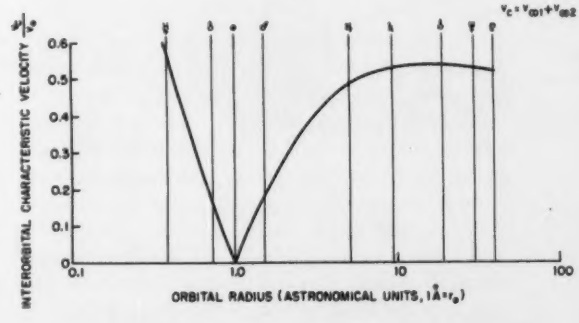

Figure 4c. Characteristic velocity for interorbital transfer from the Earth's orbital radius

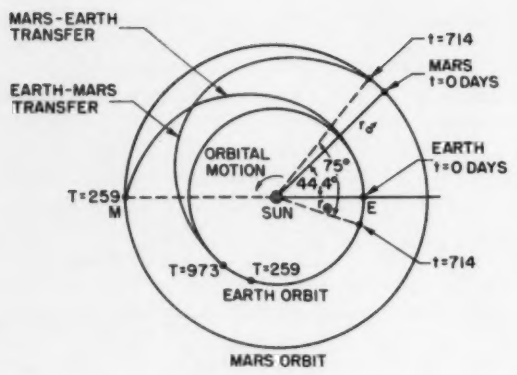

Figure 5. Ideal cotangential Earth-Mars voyage

TABLE IV

IDEAL CHARACTERISTIC VELOCITY REQUIREMENTS AND TRANSFER TIME FOR INTERPLANETARY TRANSFER

	☿	♁	♂	♃	♄	♅	♆
♁	22,010[1] 18,950[2] 26,060[3] 38,540[4] 75.5[5]	♁					
⊕	31,520 24,705 34,350 44,200 105.5	8,880 8,190 34,710 37,710 146	⊕				
♂	41,270 28,760 43,470 33,260 170.5	18,910 15,645 38,514 22,890 217.5	9,655 8,685 37,895 18,830 259	♂			
♃	57,206 26,890 58,810 624,840 853	37,355 21,675 50,210 624,635 931.3	28,830 18,500 46,625 624,535 997.3	19,230 13,906 25,475 624,415 1,126	♃		
♄	60,660 22,790 62,180 121,200 2,018	41,760 19,760 53,570 120,670 2,122	33,730 17,845 49,810 120,370 2,209	24,710 14,985 29,830 119,980 2,375	5,890 5,050 624,290 119,145 3,654	♄	
♅	62,825 17,870 64,290 72,180 5,589	44,615 16,295 55,820 71,810 5,733	36,980 15,280 52,065 71,585 5,853	28,500 13,705 33,030 71,265 6,082	10,885 7,730 624,355 70,360 7,774	4,920 4,120 119,140 70,055 9,937	♅
♆	63,615 14,975 65,065 80,270 10,845	45,670 13,960 56,670 80,085 11,025	38,205 13,290 52,940 79,970 11,174	29,956 12,246 34,300 79,805 11,458	13,085* 8,135 624,400 79,280 13,517	7,335 5,445 119,265 79,050 16,086	2,345 2,095 69,975 78,890 22,306

[1] V_∞ at inner planet (ft/sec)
[2] V_∞ at outer planet (ft/sec)
[3] V_{c0} at inner planet surface (ft/sec)
[4] V_{c0} at outer planet surface (ft/sec)
[5] transfer time (days)

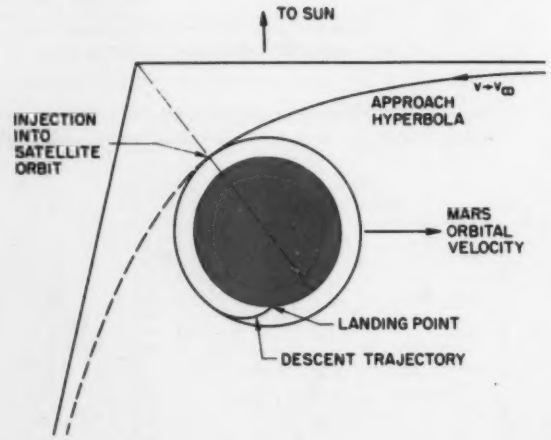

Figure 6a. Hyperbolic approach of Earth-Mars transfer

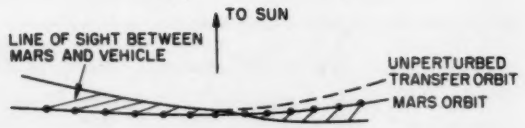

Figure 6b. Mars approach in solar coordinates illustrating perturbation due to planet

could then be reduced by an order of magnitude. A transfer orbit using nuclear-electric propulsion would not be elliptical, but could be represented by a logarithmic spiral since the vehicle would experience a low level thrust acceleration throughout most of the transfer.

Planetary Approach

As the vehicle moves outward along the transfer ellipse, its velocity decreases in the manner predicted by the vis-viva Equation 7. The vehicle thus initially moves ahead of the Earth and Mars; however, as the vehicle approaches Mars its velocity falls off until it is overtaken by the planet. In Mars-centered coordinates, therefore, the vehicle appears to approach in a direction opposite to the orbital motion as shown in Figure 6. As the vehicle nears the planet, it could enter a satellite orbit about the planet or land on the surface using reaction thrust or atmospheric drag. The analysis of the satellite orbit entry and the powered landing are simply the reverse of the Earth departure, however, atmospheric braking differs in that it is possible, in principle anyway, to obtain the requisite energy from the atmosphere.

Summary

Interplanetary flight in rudimentary form was attempted by the Soviet Union with their Venus Probe in 1961, and, even though the mission was not entirely successful, it serves as an indication of what may be accomplished in the next few decades. The path followed by the vehicle mentioned above as well as any other space craft can be represented with reasonable accuracy as a succession of orbits, each under the influence of a single attracting center. Any degree of refinement desired can be obtained by introducing the effects of other bodies as perturbations on the basic orbit or by analyzing the multi-body problem. Since general solutions to the relative motion of three or more bodies are mathematically impossible, numerical integration techniques must be used in the analysis, precluding simple motion along a conic section in these cases.

When the simplified two-body model—space vehicle and attracting center—is used, useful analytical results can be obtained for determining the over-all mission requirements. These results are obtained in the form of characteristic velocities (v_{ci}) required to perform various maneuvers associated with the mission. These characteristic velocities are then used to establish the vehicle size and staging arrangement when introduced into the basic equation of rocket-powered motion

$$v_{ci} = \sum_{j=1}^{n_i} C_{ij} \ln R_{ij} \quad , \qquad (16)$$

where C_{ij} and R_{ij} are the vehicle exhaust velocity and mass ratio, respectively, and the indices i and j refer to the particular maneuver and staging arrangement, respectively.

TABLE V

MISSION REQUIREMENTS FOR EARTH-MARS TRANSFER

MANEUVER	CHARACTERISTIC NO BRAKING	VELOCITIES BRAKING
Earth-Mars		
Earth escape (v_{co} at $r_\oplus$)*	37,985	37,985
Gravity and aero loss (20%)	7,600	7,600
Mars landing (v_{co} at $r_{\sigma'}$)*	18,830	0
Gravity and aero loss (7%)	1,320	0
Mars-Earth		
Mars escape (v_{co} at $r_{\sigma'}$)*	18,830	18,830
Gravity and aero loss (10%)	1,883	1,883
Earth landing (v_{co} at $r_\oplus$)*	37,985	0
Gravity and aero loss (8%)	3,040	0
Overall allowance for error correction	2,000	1,500
Total v_{co} for round trip mission	133,073	67,798

$r_\oplus$ = radius of Earth
$r_{\sigma'}$ = radius of Mars
Loss factors selected from empirical data
*See Table IV.

The basic maneuvers for interplanetary flight are 1) escape from the parent planet along a planetocentric hyperbola such that the vehicular velocity at some great distance from the planet ($r = \infty$ effectively), when added to the planet's orbital velocity, satisfies the conditions for entry into the desired transfer ellipse, 2) free-fall motion in a heliocentric transfer ellipse that intersects the orbits of the parent and target planets, and 3) approach to the target planet along a planetocentric hyperbola from which a landing or satellite entry maneuver is possible.

The mission requirement is expressed as the sum of the characteristic velocities for the maneuvers. The use of aerodynamic braking will alter the total velocity requirement and introduce differences in the outgoing and return values. Using the Earth-Mars transfer as an example, Table V illustrates mission requirements with and without aerodynamic braking. With the technique outlined in this table, it is possible to obtain approximate estimates for general interplanetary requirements that are adequate for preliminary design.

Space flight holds a rather unique position in the technological time scale in that it represents the one science whose theoretical development preceded its application by several centuries. The behavior of a space craft under the influence of gravitational forces is predictable within the accuracy limits of observational and computational techniques and can be represented by a series of smoothly connected conic sections, each having a different focal point. The requirements for interplanetary transfer are obtained by determining the velocity increments necessary to produce a continuous trajectory, made up of conics, that satisfies specified end conditions. These requirements were well known in Newton's era and, it is only in recent years, that technology has advanced to the point where vehicles can be designed to meet these requirements and elevate the concept of interplanetary flight from fiction to fact. ■

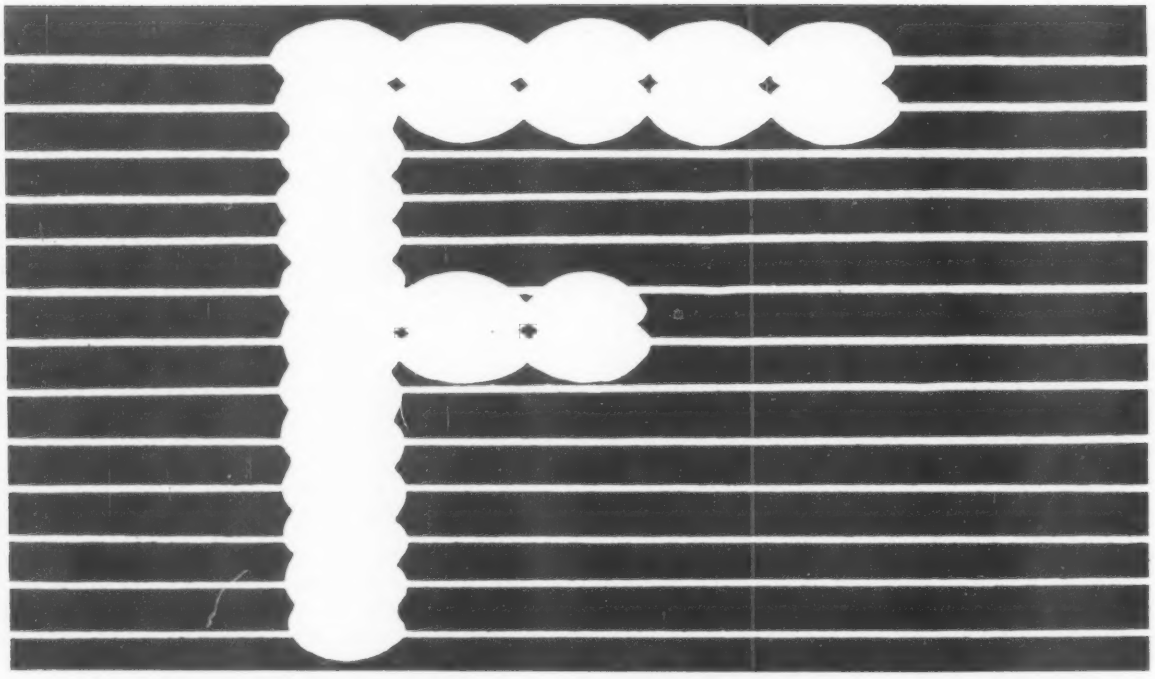

A SYMBOL GENERATOR FOR AIR TRAFFIC CONTROL

by RAYMOND W. DANKWARDT

The symbol generator described in this article won the award for the "best Canadian-designed new product exhibited at the 1961 IRE Canadian Electronics Conference."

Increasing volume and speed of air traffic makes it necessary to provide an aircraft controller with a complete radar picture of all aircraft in his area, and with a means for identification of these aircraft. Raytheon Canada Limited has developed for the Canadian Department of Transport a symbol generator to be used with bright display equipment. Scan converters in the latter equipment obtain radar information from air traffic control radars and present it to television monitors. Television-type alpha-numeric symbols are produced in the symbol generator and are displayed simultaneously with the radar information for the purpose of target identification.

A block diagram of the generator is shown in Figure 1. The position of any symbol is controlled by a joystick. Direct voltages proportional to the horizontal and vertical displacements of a joystick pass to the delay generators. These produce horizontal and vertical triggers which are delayed in time relative to the television sync pulses used to synchronize the system. The delayed horizontal trigger positions the symbol along a TV line while the delayed vertical trigger selects the line in the TV raster on which the symbol first appears.

The delayed vertical trigger opens a gate permitting a three-stage binary counter to count off the seven TV lines on which the symbol is to be displayed. The output of the counter is decoded and these decoded outputs form one set of inputs to a symbol matrix.

The delayed horizontal trigger is shaped and amplified and used to drive a tapped delay line. The output from the delay line is a series of five pulses separated in time by intervals of 0.2 μsec. These pulses form a second set of inputs to the symbol matrix.

Some, or all of these five very short pulses are transmitted on each of seven consecutive TV lines forming a symbol which is displayed on the TV monitor. The pattern is determined by a symbol matrix which is set to select dots which will make up the required letter or number. The matrix is a printed circuit board on which a number of diodes and resistors have been arranged to form a series of AND and OR gates.

A complete matrix would normally consist of 35 elements arranged in seven rows of five elements each. However, thirty-five elements is considerably greater than that required to generate a number or letter. In this system the symbols have been restricted to a maximum of 23 elements. The selection and positioning of particular elements to form an alpha-numeric is done with jumpers on the symbol matrix card. In the present system the symbol is written twice in each TV frame and the two fields of the frame are interlaced as in the title display.

In addition to the identification facility, two other features have been incorporated in the equipment. The first of these is called Hand-On. Although the personnel at a given Air Traffic Control centre may all be using the same radar, the information on their displays will be obtained from several separate scan converters. For example, one of these scan converters may be off-centred to display traffic to the east of the airport while a second scan converter will display traffic to the west of the airport. Under these conditions, and assuming that a given target is visible simultaneously on both the east and the west sector displays, the target will appear at two different positions on the respective monitor screens. The hand-on feature positions an identification symbol against a target on an east sector display, for example, which is repeated on the west sector display so that responsibility may be transferred to the west sector operator with a minimum of ambiguity and conversation.

The second feature is a Cursor. Two symbols, a cross and a rectangle, are used to measure range and bearing. The cross can be placed over any point by means of a joystick. Calibrated range and azimuth controls are provided and these set the range and azimuth of the rectangle relative to the cross. If an operator wishes to direct an aircraft to a particular spot and to predict its time of arrival or assign a ground speed, he will set one symbol over the spot (visible as map signal) and the other over the target and he can then read range and bearing to the pilot. This feature will be useful for directing lost aircraft, or assisting pilots to avoid terrain or storms. ■

RAYMOND W. DANKWARDT *was born in Kitchener, Ontario, and obtained his B.Sc. in mathematics and physics from the University of Western Ontario in 1953. After working on television receiver design at Dominion Electrohome Industries Ltd., Kitchener, he joined Raytheon Canada in 1958, and has been designing radar displays.*

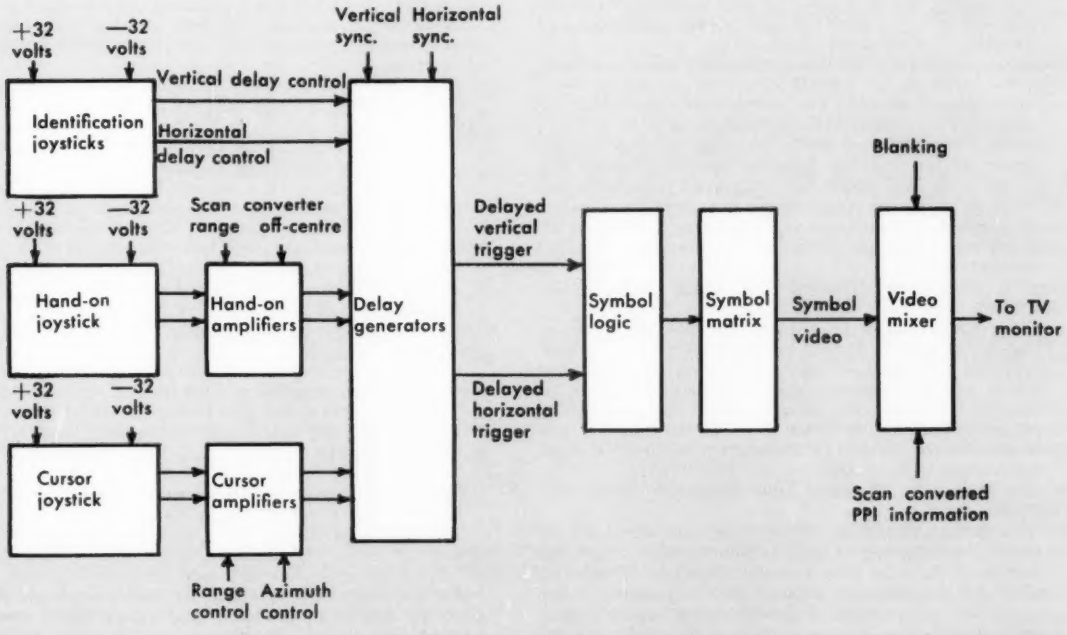

Figure 1. TV symbol generator

INVENTIONS

PATENT DISCLOSURES by the following personnel have been approved for filing.

CHARLES J. BARDSLEY,
THEODORE C. TAYLOR . . Selective Melting of Semiconductive Bodies
ALEX L. MACDONALD . . . . . Method of Doping
WILHELM RINDNER . . . . . A Semiconductor Reactance
WILHELM RINDNER . . . . . A Magnetically Controlled Semiconductor Diode
ERNST SCHLOEMANN . . . . . Adjustable Delay Line
STANISLAW G. SCHROTER . . Control of Electrophoretic Coating
WARREN J. SMITH . . . . . Fiber Bundle Amplitude Tracker
TREVOR TEMPLE . . . . . Transistor Oscillator

PATENTS

ABSTRACTS OF RAYTHEON PATENTS issued during September and October, 1961. The following are abstracts of the technical content of the patents and do not necessarily reflect the scope of coverage being claimed. Copies of the patents may be obtained through Raytheon's divisional libraries.

ROBERT A. FRYKLUND, "Echo Ranging Devices," Patent No. 3,001,190

This patent relates to an information display system, such as a solar system, in which information with respect to bearing angle, range and depth of a target is provided on the face of a single scope such as a cathode ray tube. Use is made of a plurality of transducers arranged in a semi-circle array and movable about a horizontal axis. The transducer outputs are picked up by a capacitor commutator and two patterns and swept on the scope face, one of which gives the plan position indication and the other of which gives depth.

ROBERT A. WATKINS, "Reticle System for Optical Guidance Systems," Patent No. 3,002,098

This patent relates to a reticle system for use in tracking targets. The system includes means, such as a Dove prism, for causing the center of image rotation and the center of the tracking field to coincide whereby the image of an axial target falls at a fixed point while the image of an off-axis target travels in a circle the diameter of which is proportional to target angle and the instantaneous position of which is proportional to target orientation angle.

SADIA S. GUTERMAN, "Digital Computing," Patent No. 3,002,183

This patent relates to a magnetic core shift register matrix for shifting signals in the horizontal or vertical direction by means of oppositely poled shift windings which actuate selective intercore delay circuits. Advantage is taken of the polarity of the shift windings as related to the polarity of the diodes in the delay circuits to provide the vertical or horizontal directional shift of information in the matrix.

RICHARD F. SPURCK, "Electron Tube Structure," Patent No. 3,003,603

This patent relates to an electron tube structure in which a sealing ring is used to join together a metallic portion of the tube with a ceramic envelope, in order to allow for the different coefficients of expansion of the metal and the ceramic. A flexible metallic ring having an L-shaped cross-section is used to join the metal to the ceramic while at the same time leaving a space between the metal and the ceramic so that clearance is provided for any differential expansion which might take place during operation of the tube.

PAUL W. STUTSMAN, "Gas Discharge Devices," Patent No. 3,004,192

This patent relates to a gaseous tube circuit arrangement in which means for damping inherent internal oscillations in the tube are connected to the grid of the tube in order to prevent firing of the tube at an undesired time. By controlling the parameters of the damping circuit, accurate control over tube firing time is achieved.

NEIL F. DAMON, "Detachable Electrical Connectors and Attaching Means Therefore," Patent No. 3,004,238

This patent relates to a detachable electrical connector, such as a snap-in test jack in which a tubular insulating bushing is formed with interior shoulders. The bushing is adapted to receive a plug member provided with tapered resilient fingers which after having slipped past the interior shoulders latch against the shoulders to retain the plug in place.

EDWARD C. DENCH, "Magnetron Oscillators," Patent No. 3,005,129

This patent relates to a microwave tube structure, such as a magnetron-type oscillator having a two terminal non-reentrant anode structure, in which a variable reactive load is coupled to the same terminal of the structure from which output energy is obtained. Variation of the reactive load may be utilized to vary the operating frequency of the tube.

CHARLES F. WINTER, JOHN E. WALSH, "Slotted Waveguide Antennas," Patent No. 3,005,984

This patent relates to a particular slot arrangement in a slotted antenna array in the form of a waveguide arranged to transmit two separate beams fed from opposite ends of the waveguide. The array also provides means for receiving two incoming waves which are fed separately to opposite ends with no intercoupling so that the antenna may be used for both transmission and reception.

ALVIN S. LUFTMAN, FRANK E. TAYLOR, JOHN A. BUCKBEE, "Storage Tube Compensation Means," Patent No. 3,007,078

This patent relates to a storage tube system in which compensation is provided to prevent overwriting, smearing or blurring of the storage tube at the center as compared to regions near the edge of the tube. This is accomplished during storage of the video information by varying the storage screen potential during each radial scan so that, in effect, the sensitivity of the storage device during the writing period is varied to compensate for variations of the intensity of each scan.

HAROLD A. ROSEN, "Feed-Through Nulling and Duplexer Systems," Patent No. 3,007,157

This patent relates to a feed-through nulling system for use with radar systems. The nulling system includes similar arms coupling the transmitter to the receiver, and coupling the antenna to the receiver, each arm including a ferrite rotator having their control magnetic fields energized in quadrature with respect to each other by a relatively low frequency signal. The unwanted feed-through mixes in the receiver with the sidebands resulting from mixing the transmitted frequency with the low frequency signal applied to the ferrites. Comparison is made between unwanted feed-through and the low frequency energizing the control magnetic fields of the ferrite to produce error signals which energize additional (second) coils associated with each of the ferrites. Magnetization of each ferrite by the error signal allows a selected phase and amplitude of the transmitted signal to be purposely applied to the receiver to cancel the unwanted feed-through.

PAPERS AND PUBLICATIONS

All papers which have been presented at scientific meetings and published in technical journals are being listed in this section of ELECTRONIC PROGRESS. In order to ensure completeness, authors are requested to advise the Secretary, Technical Publications Panel (Lexington X240) when papers are accepted for presentation and publication.

Papers Presented at Scientific Meetings

American Rocket Society Space Flight Report to the Nation, New York City, N.Y., October 9-15, 1961

C. C. ABT, Missile and Space Division, "The Problems and Possibilities of Space Arms Control."

Conference on Magnetism and Magnetic Materials, Phoenix, Arizona, November 13-16, 1961

J. H. SAUNDERS, J. J. GREEN, Research Division, "Subsidiary Absorption Effects in Ferrimagnetics." I. BADY, E. SCHLOEMANN, Research Division, "Onset of Spin-Wave Excitation in Planar Ferrites." L. RIMAI, G. A. DEMARS, Research Division, "Paramagnetic Resonance of Gd in Yttrium Gallium Garnet." E. A. MAGUIRE, J. J. GREEN, Research Division, "Magnetic Properties of Yttrium-Gadolinium-Aluminum-Iron Garnets." J. J. GREEN, E. SCHLOEMANN, Research Division, "Investigation of Spin-Wave Interaction by the Parallel Pumping Techniques."

Conference on Reliability Assurance Techniques for Semiconductor Specifications, Washington, D.C., October 25-26, 1961

M. PRENDERGAST, Semiconductor Division, "Common Sense in Sampling."

Eighth Annual East Coast Conference on Aerospace and Navigational Electronics, Baltimore, Md., October 23-25, 1961

C. C. ABT, Missile and Space Division, "Planning, Design, and Evaluation of Command and Control Systems." W. W. SHRADER, Equipment Division, "Results of Antenna Pattern Considerations." W. BRANDON, Missile and Space Division, "The Influence of Atmospheric Attenuation of Millimeter Waves on a Satellite Telemetry System."

New England Spectrographic Society Meeting, Chestnut Hill, Mass., November 8, 1961

E. B. BOYCE, Industrial Components Division, "Quantitative Problems in Emission Spectroscopy."

1961 Fall URSI-IRE Meeting, Austin, Texas, October 23-25, 1961

L. C. EDWARDS, G. D. THOME, Equipment Division, "Sudden Frequency Shift Observed at High Frequency During Ionospheric Disturbances." H. HOOGANIAN, D. B. ODOM, J. F. ROCHE, Equipment Division, "Investigation of Variations in the Ionosphere with the Use of Phase Coherent Backscatter Techniques."

1961 Electron Devices Meeting, Washington, D.C., October 26-27, 1961

H.-J. KRAHN, Microwave and Power Tube Division, "Investigation and Evaluation of Two New Non-Planar Ladder Derived Delay Lines." P. W. STUTSMAN, R. N. KING, C. F. HEINLEIN, JR., Industrial Components Division, "A Grid-Controlled Cold Cathode Visual Indicator."

Ninth Weather Radar Conference, Kansas City, Mo., October 23-26, 1961

A. BAUMANN, Equipment Division, "Meteorological Radars and Special Applications."

19th U.S. Navy Symposium on Underwater Acoustics, Washington, D.C., November 13-15, 1961

J. K. EASTON, B. E. MCTAGGART, N. SEROTTA, Equipment Division, "A Transducer System for the AN/AQS8(XN-2) Sonar Set." (Confidential). S. WISOTSKY, Equipment Division, "Hydroacoustic Transducer." (Confidential).

Northeast Electronics Research and Engineering Meeting (NEREM), Boston, Mass., November 14-16, 1961

C. F. LUCK, JR., R. A. PAANANEN, H. STATZ, Research Division, "Some Properties of a Gaseous Optical Maser." J. M. LAVINE, Research Division, Chairman, Tunneling Session. W. BERNARD, Research Division, "Tunneling in Esaki Diodes—A Survey Including New Effects." H. E. BLANTON, Executive Offices, R. M. JACOBS, Sylvania Electric Products Inc., "A Survey of Techniques for Analysis and Prediction of Equipment Reliability." W. C. DUNLAP, Research Division, "Trends and Topics in New Materials." W. C. BROWN, Microwave and Power Tube Division, "The Cross-Field Approach to Microwave Superpower." W. RINDNER, J. M. LAVINE, Research Division, "Scribe- and Trace-Plating: New Techniques for Microelectric Semiconductor Devices." G. WADE, Research Division, Chairman, Microwave Solid-State Devices I Session. H. STATZ, Research Division, "Generation of Coherent Light." O. T. FUNDINGSLAND, Executive Offices, Panel Member, Dynamics of Research and Development.

Seventh Radio Interference Reduction Conference, Chicago, Ill., November 7-9, 1961

R. M. COWGILL, Electronic Services Division, "Radio Interference Reduction and Spectrum Utilization in Field Army Radio Relay Systems."

Publications in Technical Journals

R. C. BARBERA, D. L. DAYTON, Missile and Space Division, "Where Direct Solar Power Conversion Stands Today" published in *International Electronics*, August 1961.

W. BEUST, W. L. FORD, Missile and Space Division, "Arcing in CW Transmitters" published in *The Microwave Journal*, October 1961.

J. R. DOW, Aero/Weapons Division, E. J. MESSNER, Industrial Components Division, "Welding for Smaller, Sturdier, Electronic Packages" published in *Space/Aeronautics*, October 1961.

M. FINIGIAN, Industrial Components Division, "High Voltage Control" published in *Electro-Mechanical Design*, October 13, 1961.

M. HOLLAND, Research Division, "Low Temperature Thermal Conductivity of Silicon" published in *Proceedings of the 1960 International Conference on Semiconductor Physics*, Prague, 1961.

G. KOSTER, M.I.T., H. STATZ, Research Division, "Probabilities for the Neon Laser Transitions" published in *Journal of Applied Physics*, October 1961.

J. M. LAVINE, W. RINDNER, B. NOST, R. NELSON, Research Division, "The Spacistor" published in *IRE Transactions on Electron Devices*, July 1961.

C. G. LEHR, I. SILBERMAN, J. W. LOTUS, Research Division, "Electron Trajectories in a Magnetron" published in *Proceedings of the 1960 International Congress on Microwave Tubes*, Munich, 1961.

A. L. MACDONALD, W. J. HEINECKE, Semiconductor Division, "Effects of Heat Treatment on Diffused Silicon Material" published in *Semiconductor Products*, September 1961.

R. PUCEL, Research Division, "Theory of the Esaki Diode Frequency Converter" published in *Solid-State Electronics*, November 1961.

C. D. ROOT, E. ADLER, Semiconductor Division, "An Introduction to the Avalanche Transistor" published in *Electro-Technology*, August 1961.

G. RUPPRECHT, Research Division, "Capture Cross Section of Surface and Bulk States in Semiconductors by Pulsed Field Effect Technique" published in *Proceedings of the 1960 Conference on Semiconductor Physics*, Prague, 1961.

S. WOLSKY, E. J. ZDANUK, Research Division, "The Interaction of Semiconductor Surfaces with Neutral and Ionized Gasses" published in *Proceedings of the 1961 Conference on Semiconductor Physics*, Prague, 1961.

TECHNICAL PUBLICATIONS PANEL

The Technical Publications Panel consists of representatives of each of the Company's major scientific and engineering activities. Their function is to seek out opportunities for technical papers and to assist authors in expediting Company review procedures. Authors are urged to contact their respective panel representatives on all such matters.

Chairman, W. E. FELLING; *Secretary*, M. A. WALKER; *Aero/Weapons Division*, G. A. HALTERMAN; *Airborne Operation*, A. DINWIDDIE; *Commercial Apparatus and Systems Division*, R. P. CURTIS; *Industrial Components Division*, A. C. RUCKWOOD; *International Services*, T. J. KELLY; *Law Department*, E. J. GORN; *Missile and Space Division*, J. W. BRODERICK, JR.; *Microwave and Power Tube Division*, W. W. TEICH; *Public Relations*, G. G. BARKER; *Receiving Tube Operation*, V. K. ULRICH; *Research Division*, H. R. BOYD; *Semiconductor Division*, D. RUBINFIEN; *Communications and Data Processing Operation*, G. PARTRIDGE; *Santa Barbara Operation*, W. TUSTIN; *Submarine Signal Operation*, L. BATCHELDER; *Surface Radar and Navigation Operation*, W. M. HALL.

ANOTHER ADVANCED MICROWAVE TUBE DEVELOPMENT
FROM RAYTHEON'S SPENCER LABORATORY

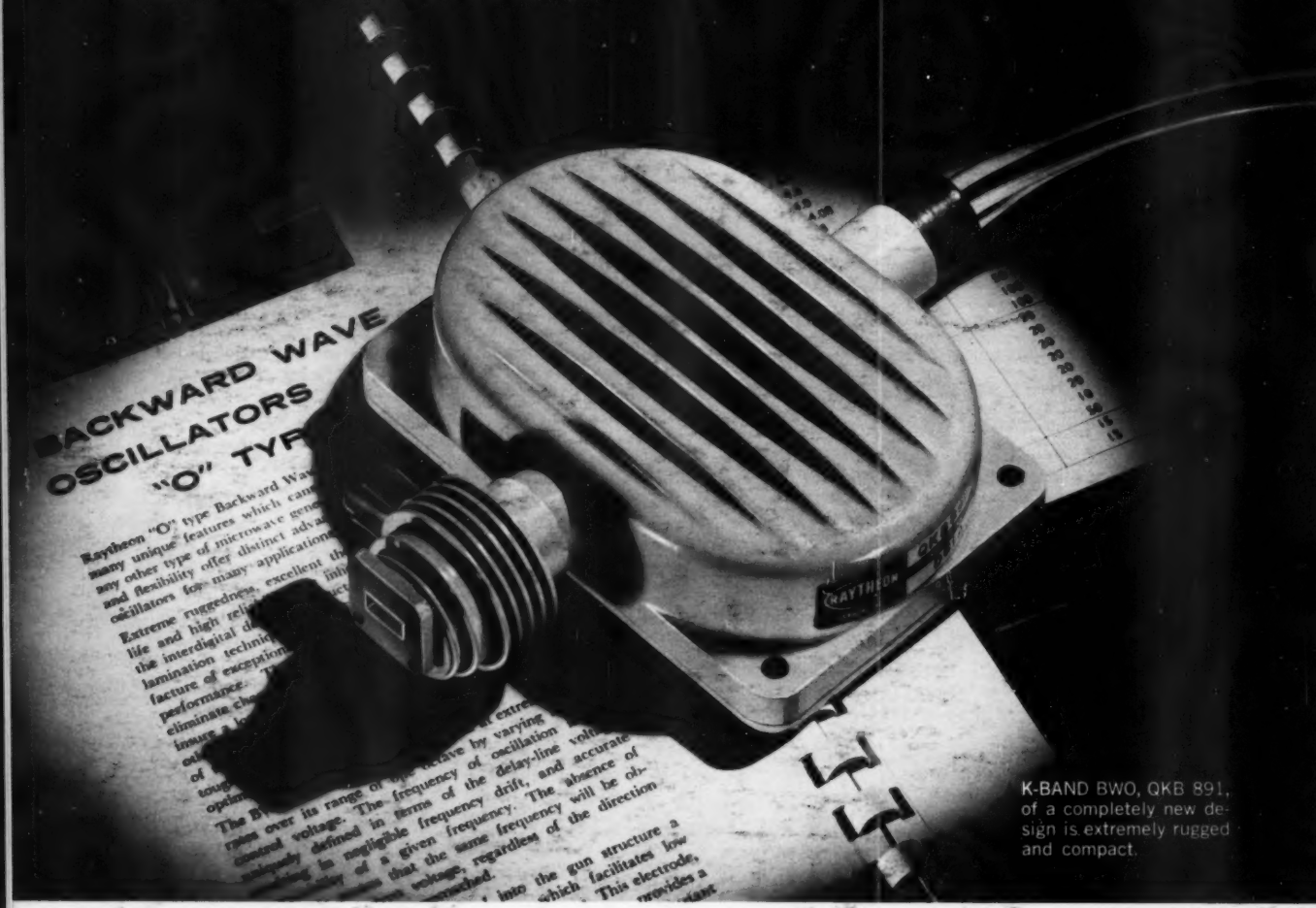

K-BAND BWO, QKB 891, of a completely new design is extremely rugged and compact.

New K-band O-type BWO's extend Raytheon compatible line to 26.5 kMc

Advanced design provides 40 mW minimum power output in extremely rugged and compact package.

Size and weight of these two new Raytheon backward wave oscillators are barely half that of units now in use.

The QKB 890 and QKB 891 are designed for such applications as swept local oscillators in ECM receivers and test equipment, driver tubes in frequency diversity radars, and pump tubes for broadband parametric amplifiers. Both tubes utilize PM focusing and have grids for low-voltage pulsed operation. For equipment designs requiring close mounting, only two-inch spacing between tubes is necessary.

Write today for detailed technical data or application service to Microwave and Power Tube Division, Raytheon Company, Waltham 54, Massachusetts. In Canada: Waterloo, Ontario.

TYPICAL OPERATING CHARACTERISTICS

	QKB 890	QKB 891
Frequency Range	12.4-18 kMc	18-26.5 kMc
Power Output	40-180 mW	40-180 mW
Delay Line (tuning)	400-1270V	600-2100V
Anode Voltage (fixed)	125V	150V
Cathode Current	17-21 mA	21-32 mA
Filament Voltage	6.3 Volts	6.3 Volts
Waveguide Coupling	RG91/U	RG53/U

RAYTHEON

RAYTHEON COMPANY

MICROWAVE AND POWER TUBE DIVISION